國　立　交　通　大　學

電 信 工 程 研 究 所

碩 士 論 文

寬頻 180°反射式數位移相器

Broadband 180° Reflection-Type Digital Phase Shifter

研究生：蘇聖智

指導教授：張志揚　博士

中華民國　九十九　年　七　月

寬頻 180°反射式數位移相器

Broadband 180° Reflection-Type Digital Phase Shifter

研 究 生 ： 蘇聖智　　Student : Sheng-Chih Su

指導教授 ： 張志揚 博士　　Advisor : Dr. Chi-Yang Chang

國 立 交 通 大 學

電 信 工 程 研 究 所

碩 士 論 文

A Thesis
Submitted to Institute of Communication Engineering
College of Electrical and Computer Engineering
National Chaio Tung University
In Partial Fulfillment of the Requirements
For the Degree of Master of Science
in
Communication Engineering
July 2010
Hsinchu, Taiwan, Republic of China

中華民國　九十九　年　七　月

寬頻180°反射式數位移相器

研究生 ： 蘇聖智　　指導教授 ： 張志揚 博士

國 立 交 通 大 學 電 信 工 程 研 究 所

摘　　要

本論文前半部提出一個中心頻率為2.5GHz 的寬頻微波岔路環。此電路利用平衡式微帶線來激發並使用一個理想反相器取代一段二分之一波長傳輸線，可使頻寬接近120%和使體積縮小為原來的50%等優點。

本論文後半部份利用前半部分的寬頻微波岔路環實現一個中心頻率為2.5GHz 的180°寬頻反射式數位移相器。不同於傳統的反射式移相器將PIN二極體加在90°混成器上，把PIN二極體加在180°混成器並將兩個PIN二極體一順偏一反偏或一反偏一順偏可得頻寬更寬以及兩個狀態介入損失相接近的180°反射式移相器。此論文全部電路以微帶線型式製作在介電係數為3.58厚度為20mil的RO4003的基板上。

Broadband 180° Reflection-Type Digital Phase Shifter

Student: Sheng-Chih Su Advisor: Dr. Chi-Yang Chang

Institute of Communication Engineering

National Chiao Tung University

Abstract

This thesis includes two parts. In the first part, the 180° hybrid ring with a center frequency of 2.5GHz and excited by the balanced microstrip line is designed. By replacing a half wavelength transmission line with an ideal phase inverter, the 180° hybrid ring exhibits a wide bandwidth of almost 120% and the size reduced for 50%.

In the second part, by using the broadband 180° hybrid ring designed in the first part, the broadband 180° reflection type digital phase shifter has been realized. Unlike the conventional reflection type phase shifter where two PIN diodes are connected to a 90° hybrid ring with the same bias condition, in the proposed phase shifter two PIN diodes are connected to the 180° hybrid ring with opposite bias condition. The proposed one can get much wider bandwidth with almost the same insertion loss in two phase states. The whole circuits in this thesis are fabricated with microstrip line on a RO4003 substrate with a dielectric constant of 3.58, a thickness of 20 mil.

Acknowledgement

誌　　謝

時間過的可真快，兩年的研究所終於要結束了，這篇論文的完成要感謝很多貴人的幫助。

首先要感謝我的指導教授張志揚博士，在老師和藹可親、不厭其煩的指導下，我學習到許多微波領域的知識並且幫助我克服了許多研究上的難題，真的由衷的感謝您。同時，我要感謝在口試時給予我許多珍貴建議的口試委員邱煥凱教授、鍾世忠教授、孟慶宗教授，使本論文得以更加完善。

接下來我要感謝 916 實驗室眾多學長姐、學弟妹以及同學的陪伴與照顧下，讓我能在充滿歡樂氣氛的實驗室下進行研究與學習。其中包括已畢業學長姐金雄、哲慶、宗傑、殿靖、如屏、耿宏以及博班學長益廷、正憲、昀緯、建育，學弟妹維欣、懿萱、鵬達、宛蓉，還有實驗室同窗德裕、姵潔、揚達、士峰。另外，也感謝求學過程中一路陪伴我的人們，謝謝你們，有你們真好。

最後，我要感謝我最親愛的父母親、弟弟，因為有你們的支持和相挺，讓我能順利的完成碩士學位，感謝你們，謝謝！

Table of Contents

List of Tables

List of Figures

Chapter 1
Introduction

A phase shifter operated at the microwave frequency is an essential element in a wide variety of applications such as phase modulators, frequency up-converters, testing instruments, and phased array antenna systems. Take phased array antenna system as an example, most antennas send or receive in all directions, but phase shifters enable phased array antennas to accumulate signal to or from specific direction. By incorporating a network of phase shifters, the beam of a phased array antenna can be pointed electronically in microseconds without any physical realignment or movement of the antenna or its elements. Designing of phase shifters should consider many factors such as phase shift, low insertion loss, low phase error, bandwidth, low insertion loss variation, simple control, low dc power consumption, high speed, small size, and low cost for commercial wireless communication. There are many types of phase shifters, such as switched-line phase shifter, loaded-line phase shifter, and reflection type phase shifter. For large phase shift, the most commonly used phase shifter is reflection type phase shifter. In this thesis, the broadband 180° reflection type phase shifter will be realized.

In chapter 2, a broadband 180° hybrid ring is proposed. By replacing the $\frac{\lambda}{2}$ line

section with the ideal phase inverter, the bandwidth of a 180° hybrid ring will be largely increased. Moreover, the overall circuit size will be reduced. The theory of the ring and the balanced microstrip line will be discussed. Design procedures, simulation and measurement results will be demonstrated as well.

In chapter 3, a 180° reflection type phase shifter applying the broadband 180° hybrid ring realized in chapter 2 will be implemented. Normally, an analog reflection phase shifter uses a 90° hybrid coupler to be connected with two varactors with the same bias condition which can exhibit maximum continuous phase shift from 0° up to 360°. However, such kind of analog phase shifter is not equal loss in all phase states. A digital phase shifter uses two PIN diodes that only two phase states can exist. Usually, the two phase states have different insertion losses. The two PIN diodes of the proposed phase shifter are connected to a 180° hybrid ring with opposite bias condition, the broadband 180° reflection type digital phase shifter with almost the same insertion loss will be achieved. The circuit analysis, design procedure, simulation and measurement results of the broadband 180° reflection type phase shifter will be presented.

Chapter 2
Broadband 180° Hybrid Ring

2.1 Introduction

The 180° hybrid ring coupler [1], which is also known as a rat-race ring, is an essential component in microwave circuits, such as balanced mixers, multipliers, push-pull amplifiers and antenna feed networks, etc. A conventional 180° hybrid ring consists of three $\frac{\lambda}{4}$ line sections and one $\frac{3\lambda}{4}$ line section as shown in Figure 2.1. The $\frac{3\lambda}{4}$ line section works as a $\frac{\lambda}{4}$ line section with a phase inverter formed by a $\frac{\lambda}{2}$ line section. Thus, the disadvantage of the conventional 180° hybrid ring is narrow bandwidth and large size. Many researches have attributed to make the bandwidth larger. Most of the approaches are realizing an ideal or broadband phase inverter.

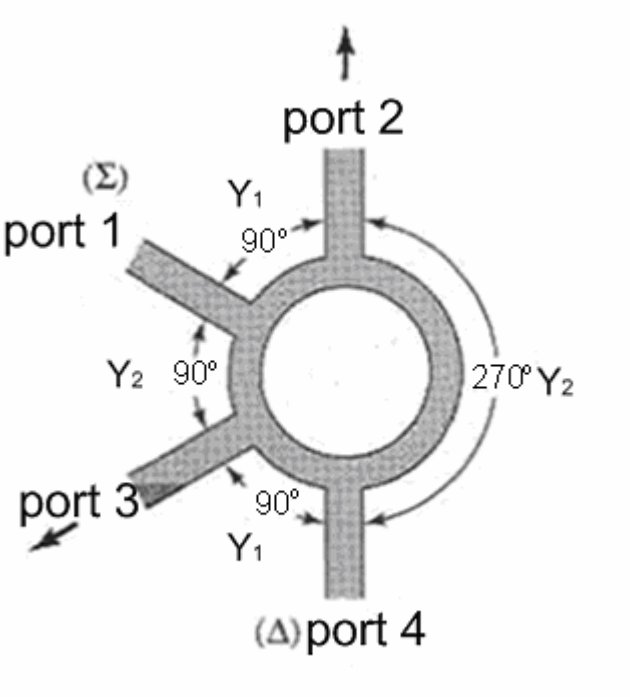

Figure 2.1: Schematic circuit of the conventional 180° hybrid ring .

In this chapter, a broadband 180° hybrid ring coupler is presented. With balanced microstrip line and an ideal phase inverter, the broadband rat-race ring has been developed.

2.2 Theory

2.2.1 Broadband 180° Hybrid Ring

The circuit schematic of a 180° hybrid ring with an ideal phase inverter [2] is shown in Figure 2.2(a). Instead of a conventional hybrid ring composed of three $\frac{\lambda}{4}$ and one $\frac{3\lambda}{4}$ line sections, the spacing between all adjacent ports is $\frac{\lambda}{4}$, and an ideal phase inverter is placed between two of the adjacent ports. With the use of an ideal phase inverter, the bandwidth of 180° hybrid ring is further increased. Even- and

odd-mode equivalent circuits of the hybrid ring are shown in Figure 2.3(a) and (b).

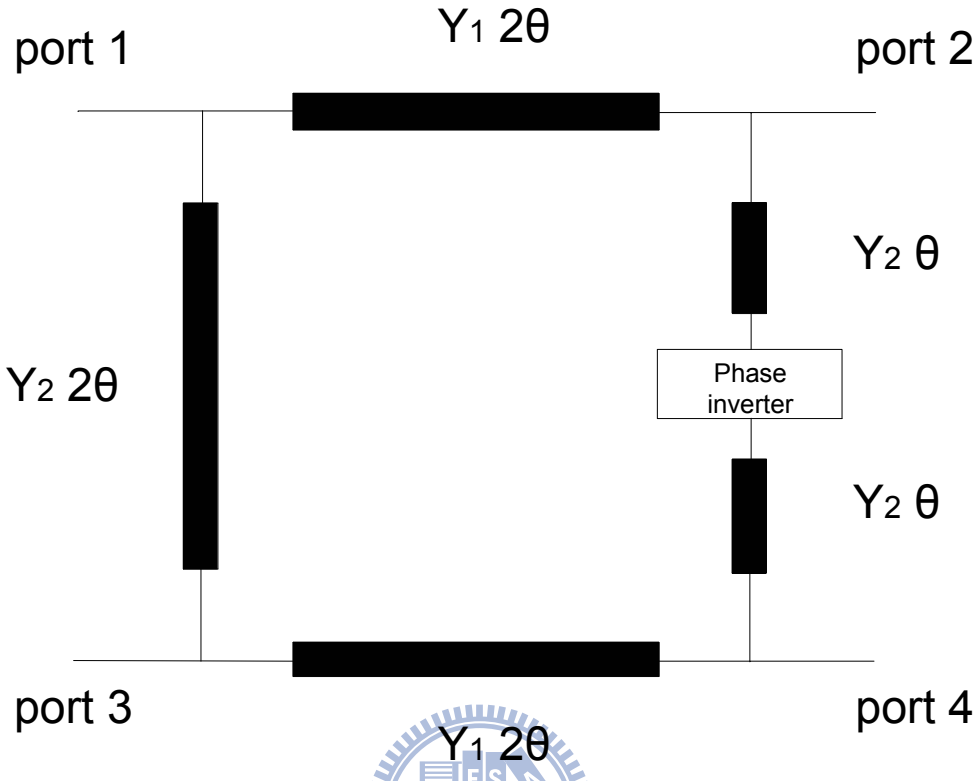

Figure 2.2: Schematic circuit of the broadband 180° hybrid ring.

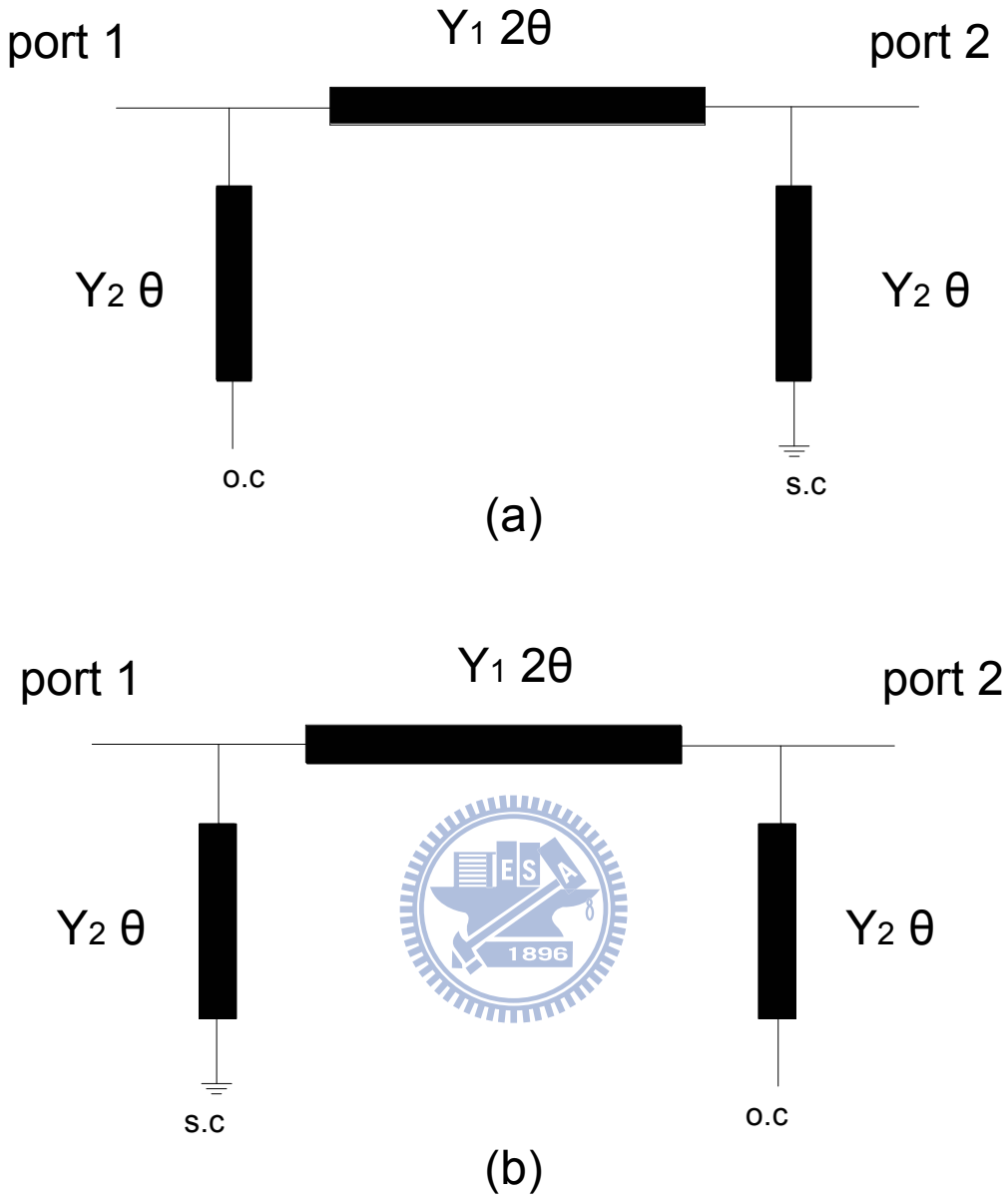

Figure 2.3: (a) Even- and (b) Odd-mode equivalent circuits of the 180° hybrid ring with an ideal phase inverter.

The ABCD matrices for the even- and odd- mode circuits are:

$$\begin{bmatrix} A_e & B_e \\ C_e & D_e \end{bmatrix} = \begin{bmatrix} 1 & 0 \\ jY_2 \tan\theta & 1 \end{bmatrix} \begin{bmatrix} \cos 2\theta & jZ_1 \sin 2\theta \\ jY_1 \sin 2\theta & \cos 2\theta \end{bmatrix} \begin{bmatrix} 1 & 0 \\ -jY_2 \cot\theta & 1 \end{bmatrix} \quad (2.1)$$

$$\begin{bmatrix} A_o & B_o \\ C_o & D_o \end{bmatrix} = \begin{bmatrix} 1 & 0 \\ -jY_2 \cot\theta & 1 \end{bmatrix} \begin{bmatrix} \cos 2\theta & jZ_1 \sin 2\theta \\ jY_1 \sin 2\theta & \cos 2\theta \end{bmatrix} \begin{bmatrix} 1 & 0 \\ jY_2 \tan\theta & 1 \end{bmatrix} \quad (2.2)$$

Y_1 and Y_2 are normalized admittance of the hybrid ring, which are normalized to

port impedance Z_0. Let θ=45° at the center frequency, then

$$\begin{bmatrix} A_e & B_e \\ C_e & D_e \end{bmatrix}_{\theta=45^\circ} = \begin{bmatrix} 1 & 0 \\ jY_2 & 1 \end{bmatrix} \begin{bmatrix} 0 & jZ_1 \\ jY_1 & 0 \end{bmatrix} \begin{bmatrix} 1 & 0 \\ -jY_2 & 1 \end{bmatrix} = \begin{bmatrix} \frac{Y_2}{Y_1} & j\frac{1}{Y_1} \\ j\frac{Y_1^2+Y_2^2}{Y_1} & -\frac{Y_2}{Y_1} \end{bmatrix} = \begin{bmatrix} A & B \\ C & D \end{bmatrix} \tag{2.3}$$

$$\begin{bmatrix} A_o & B_o \\ C_o & D_o \end{bmatrix}_{\theta=45^\circ} = \begin{bmatrix} 1 & 0 \\ -jY_2 & 1 \end{bmatrix} \begin{bmatrix} 0 & jZ_1 \\ jY_1 & 0 \end{bmatrix} \begin{bmatrix} 1 & 0 \\ jY_2 & 1 \end{bmatrix} = \begin{bmatrix} -\frac{Y_2}{Y_1} & j\frac{1}{Y_1} \\ j\frac{Y_1^2+Y_2^2}{Y_1} & \frac{Y_2}{Y_1} \end{bmatrix} = \begin{bmatrix} D & B \\ C & A \end{bmatrix} \tag{2.4}$$

The S parameters of the four-port network are:

$$S_{11} = S_{22} = \frac{B-C}{A+B+C+D} = \Gamma \tag{2.5a}$$

$$S_{21} = S_{12} = \frac{2}{A+B+C+D} = \mathrm{T} \tag{2.5b}$$

$$S_{31} = \frac{A-D}{A+B+C+D} = \frac{2(\frac{Y_1}{Y_2})}{A+B+C+D} \tag{2.5c}$$

$$S_{42} = \frac{D-A}{A+B+C+D} = \frac{-2(\frac{Y_1}{Y_2})}{A+B+C+D} \tag{2.5d}$$

The output power division ratio is:

$$R = \frac{|S_{31}|^2}{|S_{21}|^2} = \frac{|S_{42}|^2}{|S_{12}|^2} = \left(\frac{Y_1}{Y_2}\right)^2 \tag{2.6}$$

By (2.5) and (2.6), the normalized admittance Y_1 and Y_2 are related to return loss and power division. The scattering parameters of the 180° hybrid ring make it useful in many applications. For example, if the 180° hybrid ring is designed for equal

power division, that is, $Y_1 = Y_2$, it can be used as an in-phase power divider or a balun. When an input signal is incident at port 1 (sum port), the power divider provides 0° in-phase equal power division between port 2 and 3, and no power reaches port 4. On the other hand, when power is incident at port 4 (delta port), the power divider provides out-of-phase power division between port 2 and 3, and no power reaches port 1.

If $Y_1 = Y_2 = \frac{1}{\sqrt{2}} Y_0$ and θ=45°, the scattering matrix for the 180° hybrid ring thus has the following form:

$$[S] = \frac{-j}{\sqrt{2}} \begin{bmatrix} 0 & 1 & 1 & 0 \\ 1 & 0 & 0 & -1 \\ 1 & 0 & 0 & 1 \\ 0 & -1 & 1 & 0 \end{bmatrix} \tag{2.7}$$

2.2.2 Balanced Microstrip Line

The input and output of our 180° hybrid ring are conventional microstrip lines. However, the ring should be excited by the balanced microstrip line [3] [4], which is also known as broadside microstrip line or parallel plate stripline.

Characteristic impedance can be computed using formulas given in [5] for the case of broad and narrow strips. In the case of electromagnetic field patterns enabling us to introduce an electrical wall in the plane of symmetry, so the structure is transformed into two series-connected microstrip lines. In other words, the

characteristic impedance of this balanced microstrip line is just double that of a conventional microstrip line with a substrate half as thick as the balanced microstrip line. Structure of the balanced microstrip line and the equivalent circuit of the conventional microstrip line are shown in Figure 2.4(a) and (b).

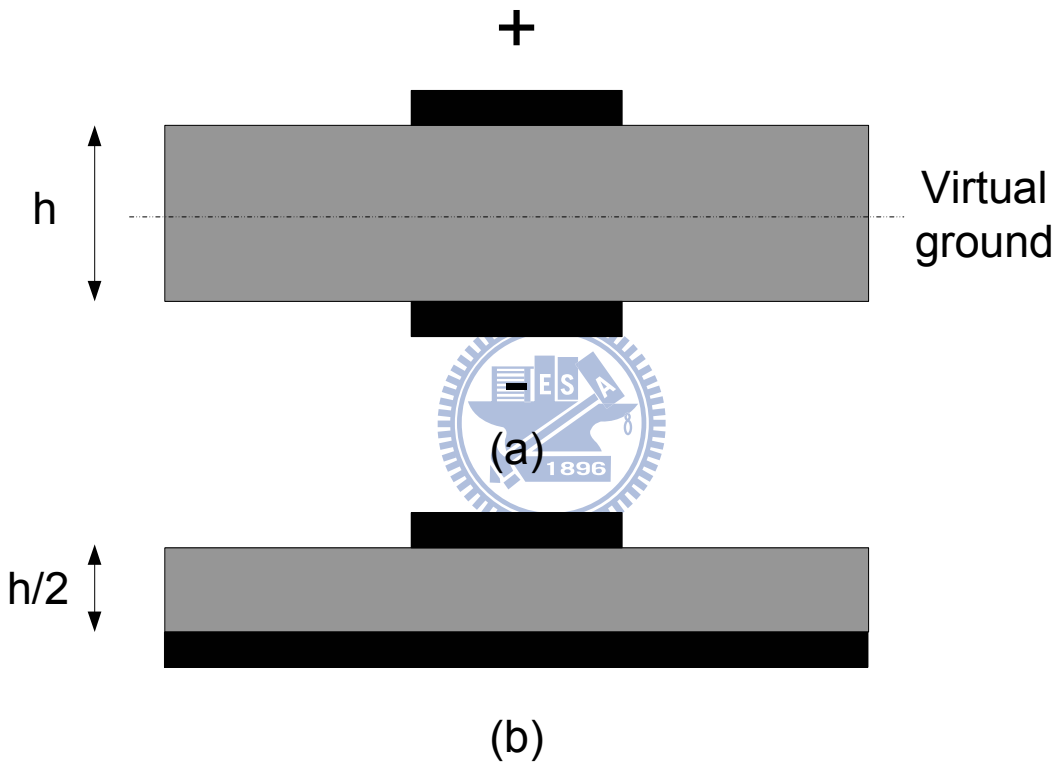

Figure 2.4: (a) The structure of the balanced microstrip line. (b) Equivalent circuit of the conventional microstrip line.

A balanced microstrip line is often used in broadband frequency with a tapered transition from microstrip line. This involves the use of a parallel plate microstrip line with different widths of strip, namely, a microstrip line with a finite ground plane width. To do this, the ground plane width of a conventional microstrip line is slowly

tapered to that of a balanced microstrip line as shown in Figure 2.5. Moreover, this microstrip to balanced microstrip line taper line must be sufficiently long to yield a well impedance-matching performance, especially in the lower frequency range. Some numerical formulas for the design of such structure can also be found in [6] and [7].

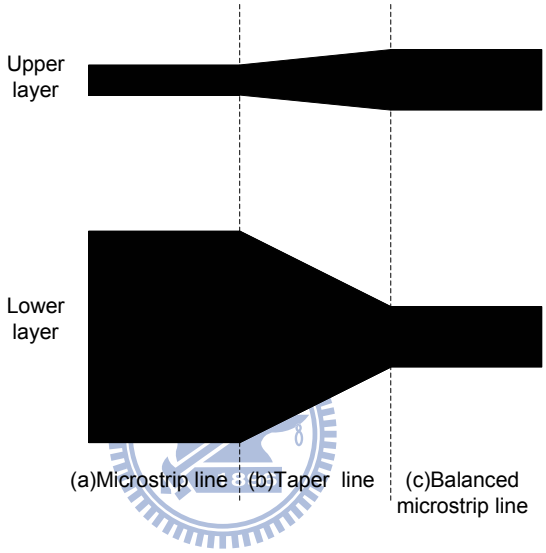

Figure 2.5: Method to transfer conventional microstrip line to balanced microstrip line.

In the inverted balanced microstrip lines, the positive (negative) strip on the upper (lower) substrate side is connected vertically through a via with the strip on the lower (upper) substrate side by the method illustrated in Figure 2.6. According to this figure, each one of the positive and negative strips is terminated by a right-angled bend in the opposite directions individually. By doing so, the positions of the positive and negative strips are exchanged upside down. It goes without saying that the balanced and inverted balanced microstrip lines are not exactly 180° out of phase,

although they have the same physical length. The electrical length of the inverted balanced microstrip line exceeds that of the balanced microstrip lines because the inverted balanced microstrip line includes an additional path that passes through the substrate which is equal to the thickness of the substrate.

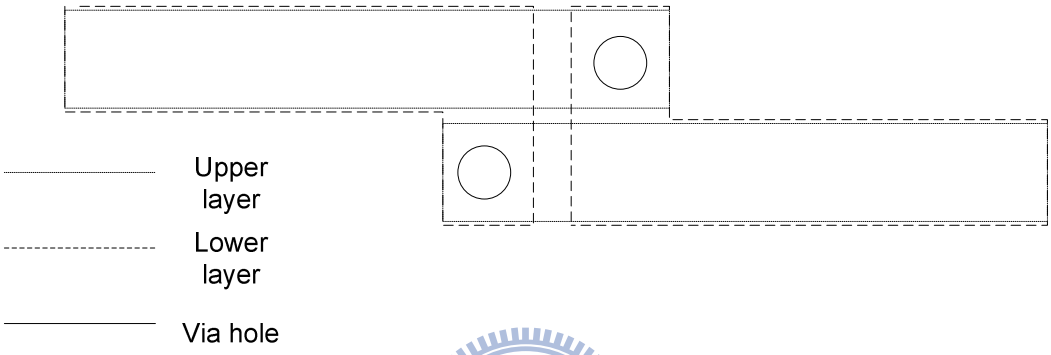

Figure 2.6: Structure of the inverted balanced microstrip line.

2.3 Design Procedure and Simulation

The entire circuit is manufactured on a Rogers RO4003 substrate with a ε=3.58 and a thickness of 20 mil. The center frequency is at 2.5GHz. To obtain the physical length of the transmission line, we use the tool, LineCalc, which is included in the commercial simulation solver Advanced Design System (ADS) of the Agilent Inc, and we utilize the 2.5D EM simulation software “Sonnet” of Sonnet Inc to complete the simulation in this study.

2.3.1 Implementation of -90° Balanced Microstrip Line

To get the physical length of the -90° balanced microstrip line, we can use the

LineCalc to compute the length of the equivalent circuit of the -90° conventional unbalanced microstrip line according to the theory mentioned before. The circuit layout of the 58Ω -90° balanced microstrip line with physical dimensions are shown in Figure 2.7 and listed in Table 2.1.The simulated phase response is shown in Figure 2.8.

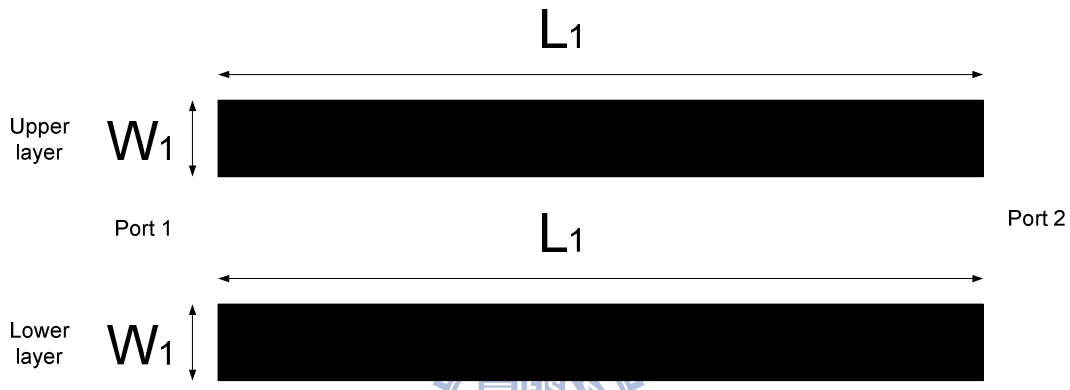

Figure 2.7: Circuit layout of the -90° balanced microstrip line.

W_1(mil)	L_1(mil)
48	681

Table 2.1: Physical dimensions of the -90° balanced microstrip line.

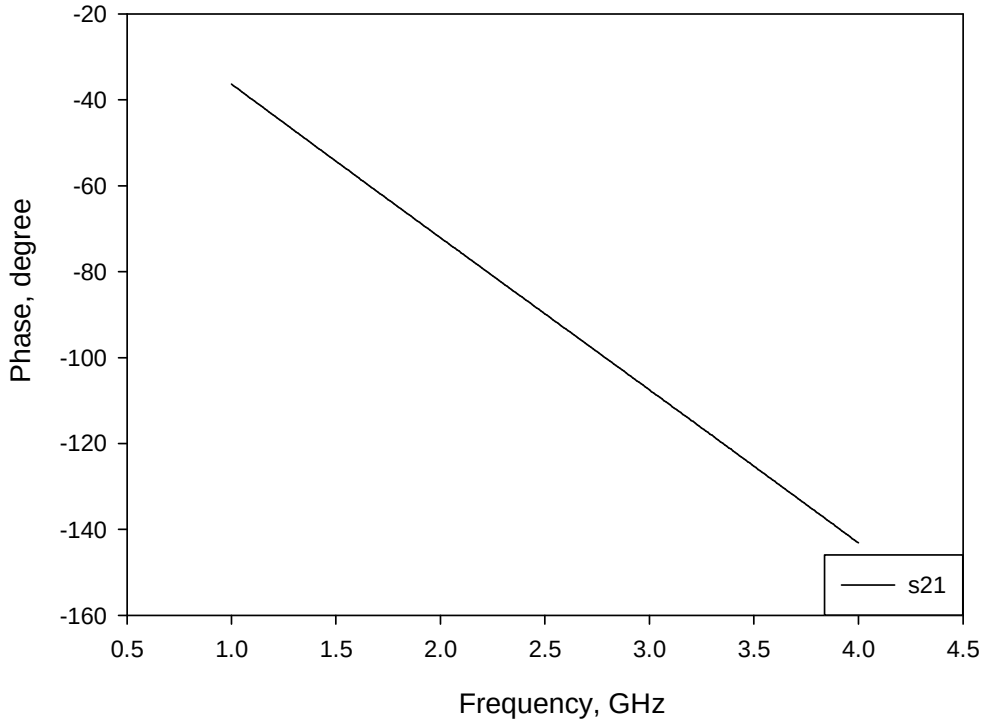

Figure 2.8: Phase response of the -90° balanced microstrip line.

2.3.2 Implementation of 90° Inverted Balanced Microstrip Line

In order to implement a 90° (-270°) balanced microstrip line, we can partition this line into two parts, a -90° section and a -180° section. The later is intended to be realized by using a structure of twist, a via connected from the top layer to the bottom layer and it is short in physical size which is equal to the thickness of the substrate. Initially, the length of the structure is made the same as that the -90° balanced microstrip line mentioned previously. In the equal physical length, the phase response at center frequency is smaller than 90°. Decreasing the physical length of the structure increases the electrical length. After fine tuning, the required 90° inverted balanced

microstrip line is obtained. The circuit layout of the 58Ω 90° inverted balanced microstrip line with physical dimensions are shown in Figure 2.9 and listed in Table 2.2. The simulated phase response is shown in Figure 2.10.

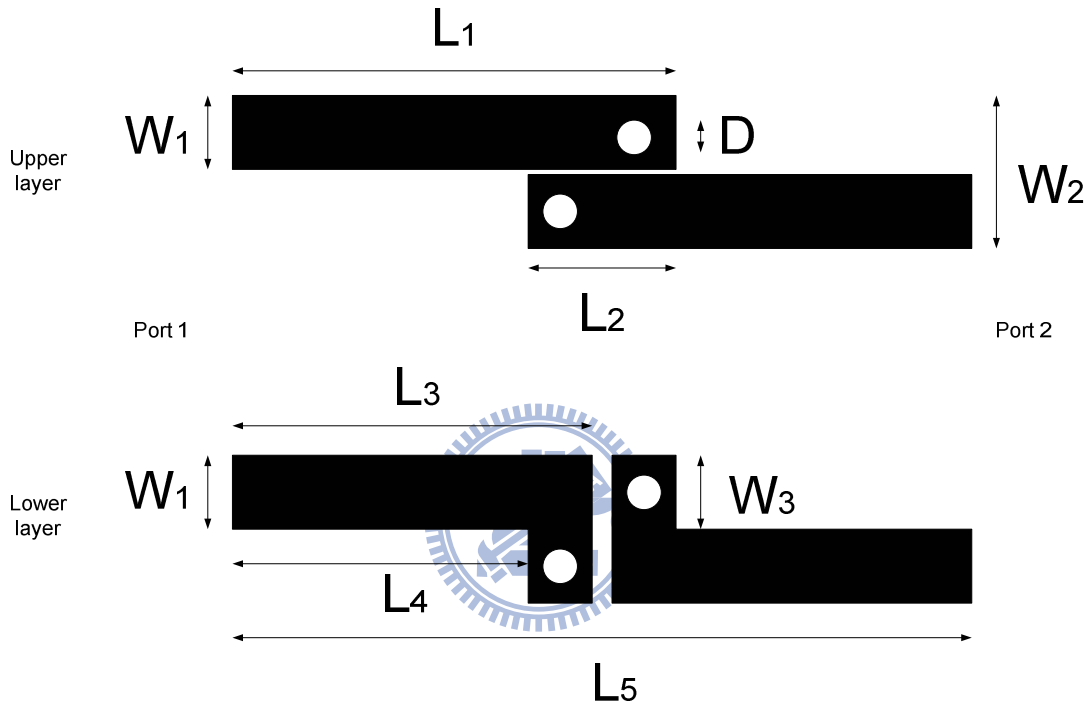

Figure 2.9: Circuit layout of the 90° inverted balanced microstrip line.

W_1(mil)	W_2(mil)	W_3(mil)	L_1(mil)	L_2(mil)	L_3(mil)	L_4(mil)	L_5(mil)	D(mil)
48	104	56	377	124	301	253	534	30

Table 2.2: Physical dimensions of the 90° inverted balanced microstrip line.

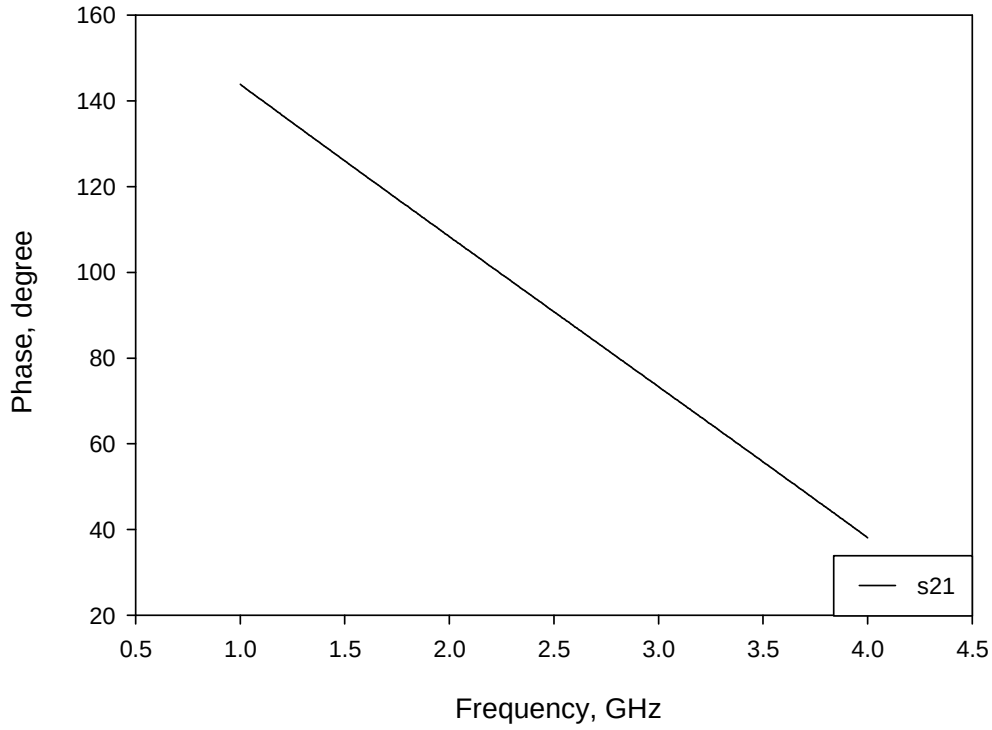

Figure 2.10: Phase response of the 90° inverted balanced microstrip line.

2.3.3 Implementation of Taper Line

A 180° ideal transformer is usually used as a microstrip to balanced microstrip line transition. However, this kind of structure is hardly achieved. A taper line shown in Figure 2.11 can alternatively be used as a transformer. The physical dimensions and the simulated result are shown in Table 2.3 and Figure 2.12, respectively. From the graph, we know that there is a 10° phase imbalance at the center frequency.

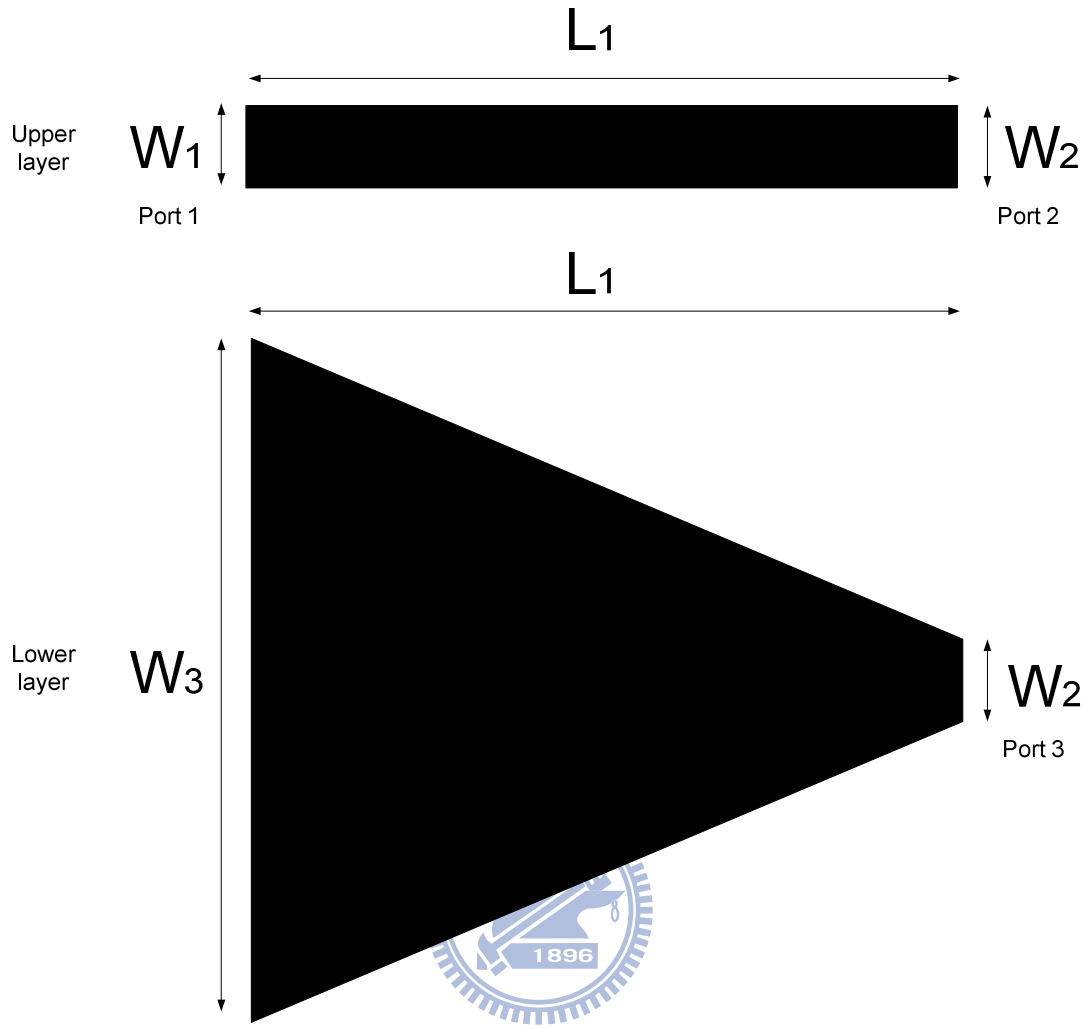

Figure 2.11: Circuit layout of the taper line.

W_1(mil)	W_2(mil)	W_3(mil)	L_1(mil)
44	48	544	545

Table 2.3: Physical dimensions of the taper line.

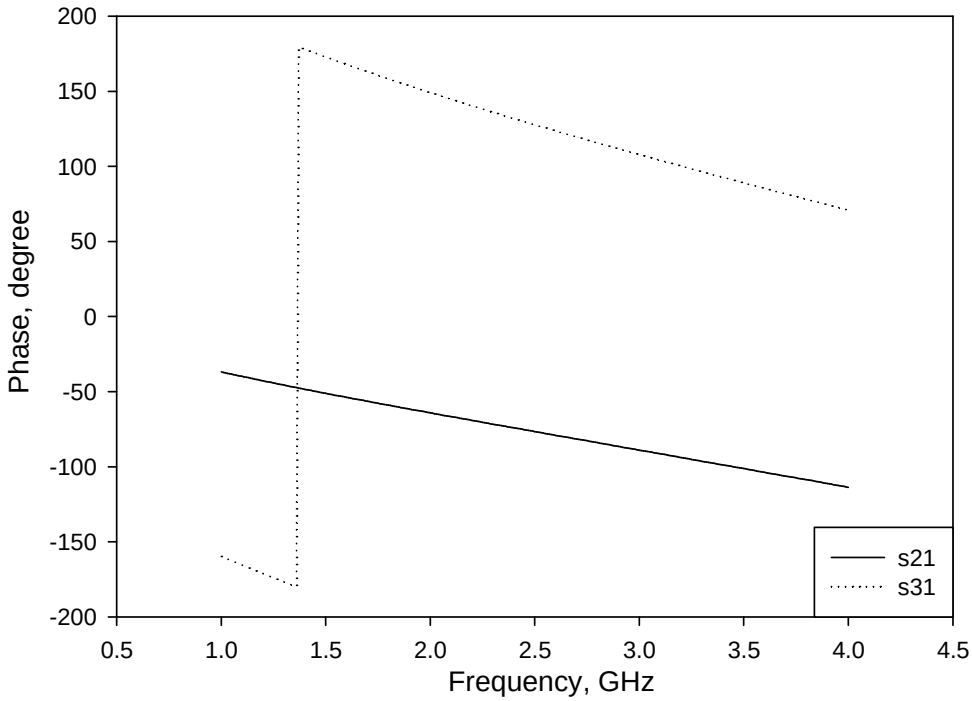

Figure 2.12: Phase response of the taper line.

2.3.4 Implementation of Broadband 180° Hybrid Ring

Now we merge the sections simulated before to become the 180° hybrid ring, including 3 sections of the -90° balanced microstrip line and one section of the 90° inverted balanced microstrip line. The 4 sections of the taper line are intended to transfer from 58Ω balanced microstrip line to 50Ω conventional microstrip line. The layout of the proposed 180° hybrid ring is shown in Figure 2.13.

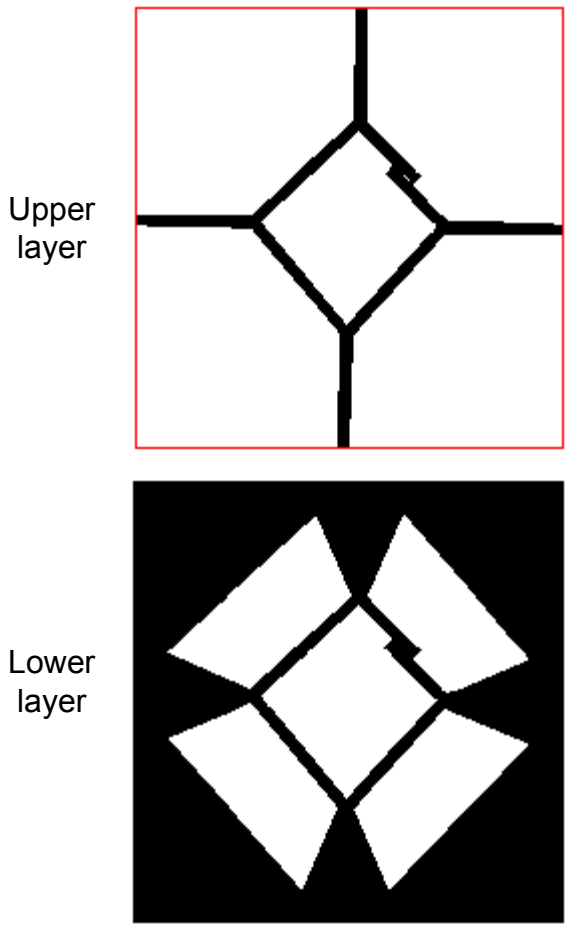

Figure 2.13: Circuit layout of the 180° hybrid ring.

The proposed 180° hybrid ring is designed to operate at 2.5 GHz, with equal power division (3dB), bandwidth from 1.5 to 3.5 GHz. The simulated passband frequency responses of the circuit for in-phase operation are shown in Figure 2.14 and Figure 2.15, and the simulated responses of the circuit for out-of-phase operation are shown in Figure 2.16 and Figure 2.17 The return loss is better than 10 dB from 1.18 to 3.82 GHz (104%) for in-phase operation and from 1.30 to 3.66 GHz (94%) for out-of-phase operation. The measured isolation is better than 25 dB in the passband for both operations. The amplitude and phase balance in the passband are less than

0.50dB and 3°, respectively, for both in-phase and out-of-phase operation.

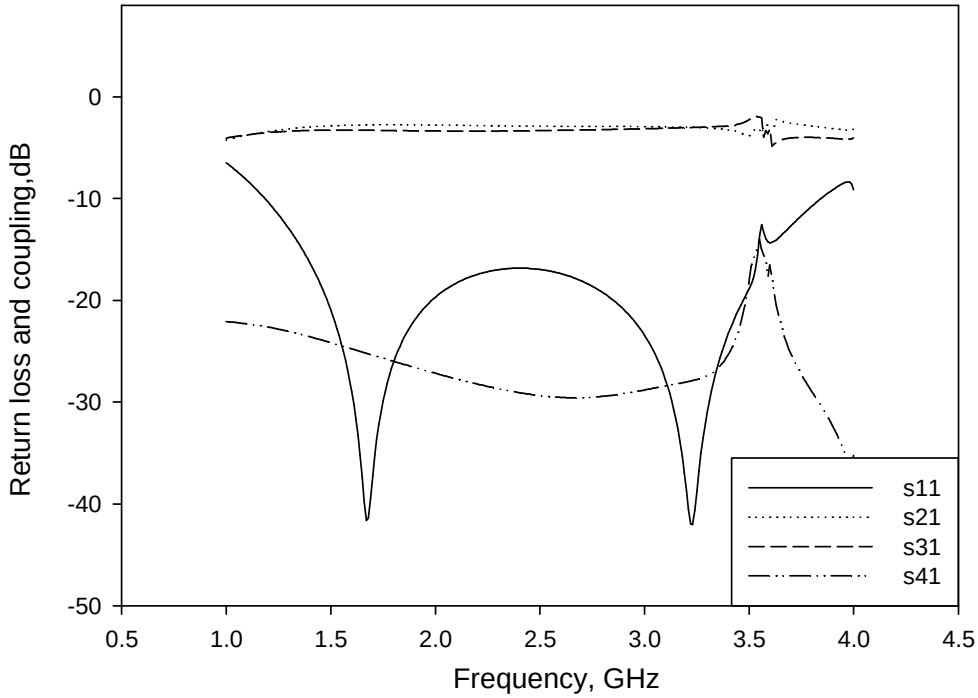

Figure 2.14: Simulated amplitude response of the 180° hybrid ring for in-phase operation.

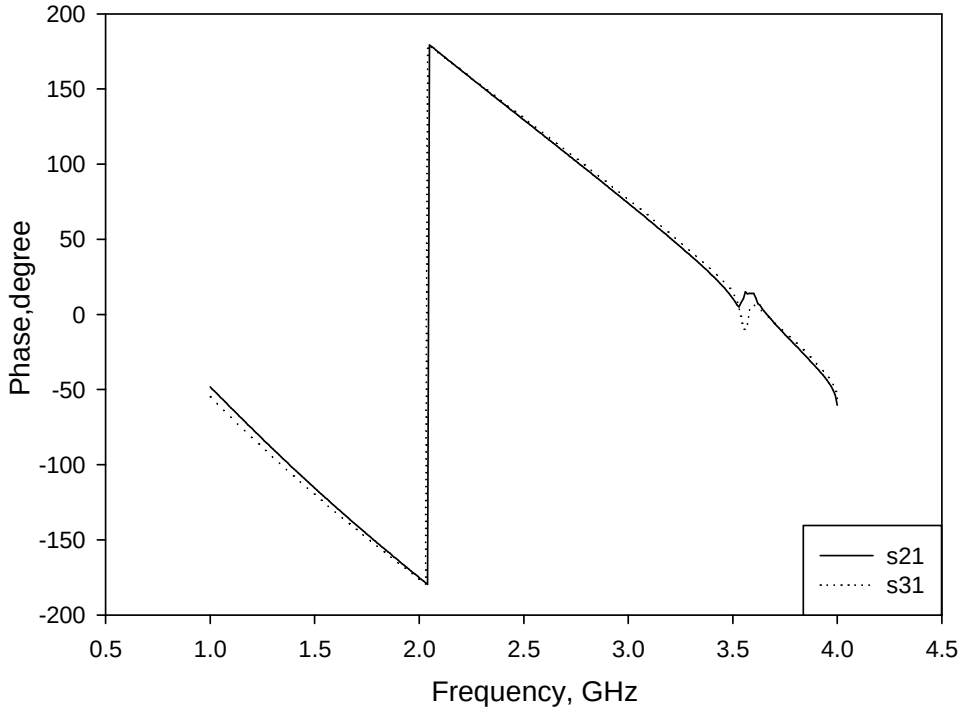

Figure 2.15: Simulated phase response of the 180° hybrid ring for in-phase operation.

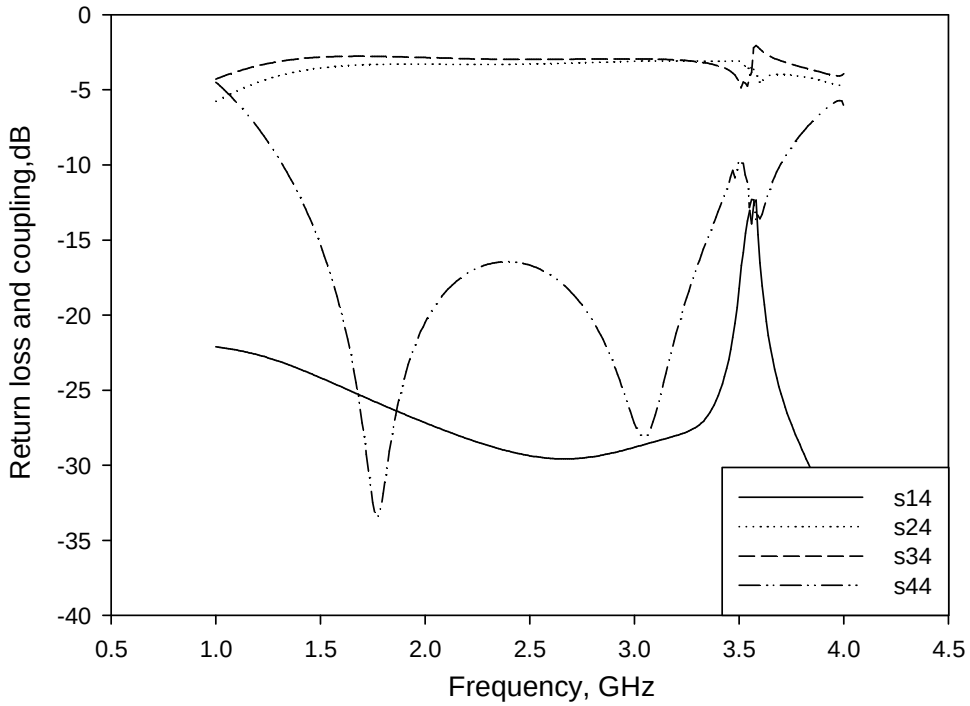

Figure 2.16: Simulated amplitude response of the 180° hybrid ring for out-of-phase operation.

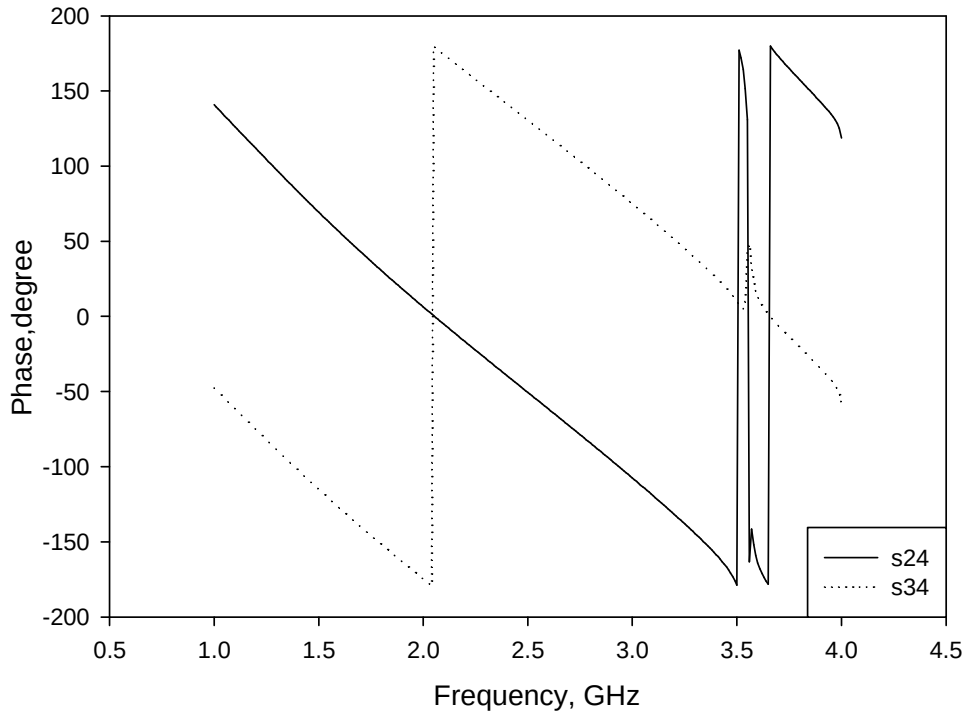

Figure 2.17: Simulated phase response of the 180° hybrid ring for out-of-phase operation.

2.4 Fabrication and Measurements

Figure 2.18 shows the photograph of designed 180° hybrid ring, of which overall circuit size is 52×52 mm^2. The measured amplitude responses of the circuit for in-phase operation are shown in Figure 2.19, and the measured responses of the circuit for out-of-phase operation are shown in Figure 2.20. The return loss is better than 10 dB from 1.10 to 4.12 GHz (120%) for in-phase operation and from 1.18 to 4.10 GHz (116%) for out-of-phase operation. The measured isolation is better than 25 dB in the passband for both operations.

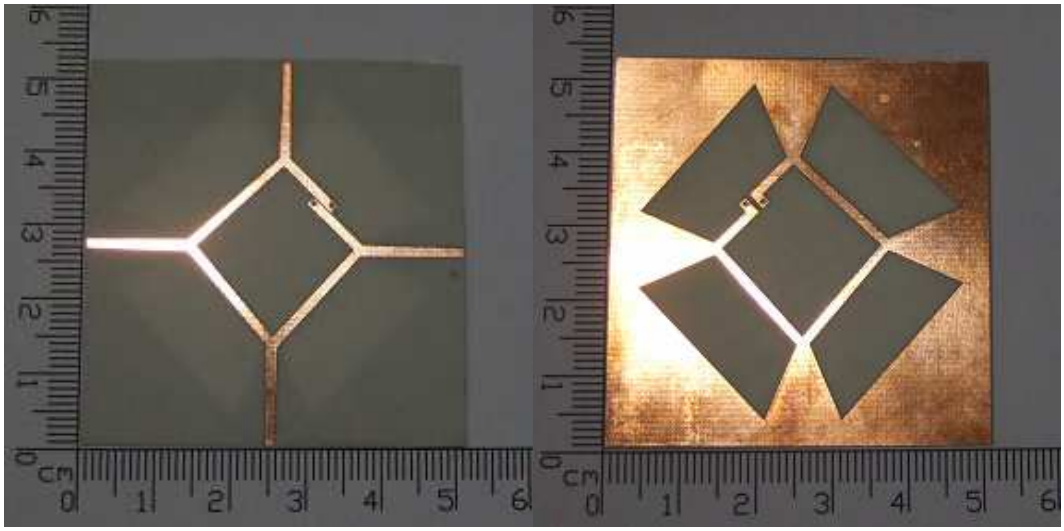

Figure 2.18: Photograph of the broadband 180° hybrid ring.

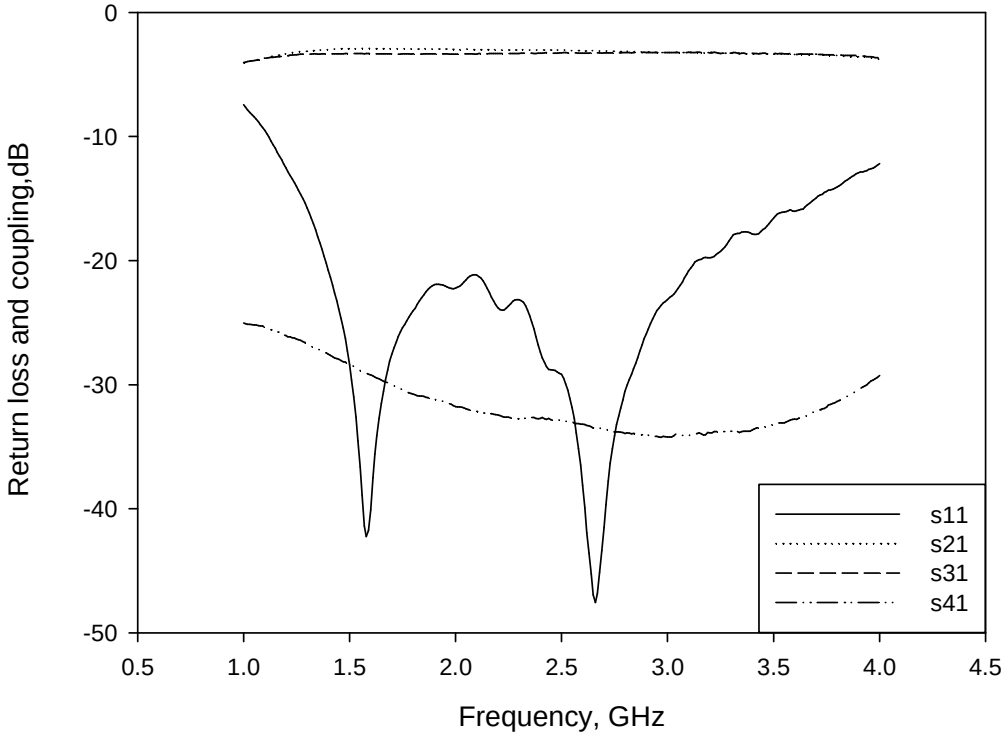

Figure 2.19: Measured amplitude response of the 180° hybrid ring for in-phase operation.

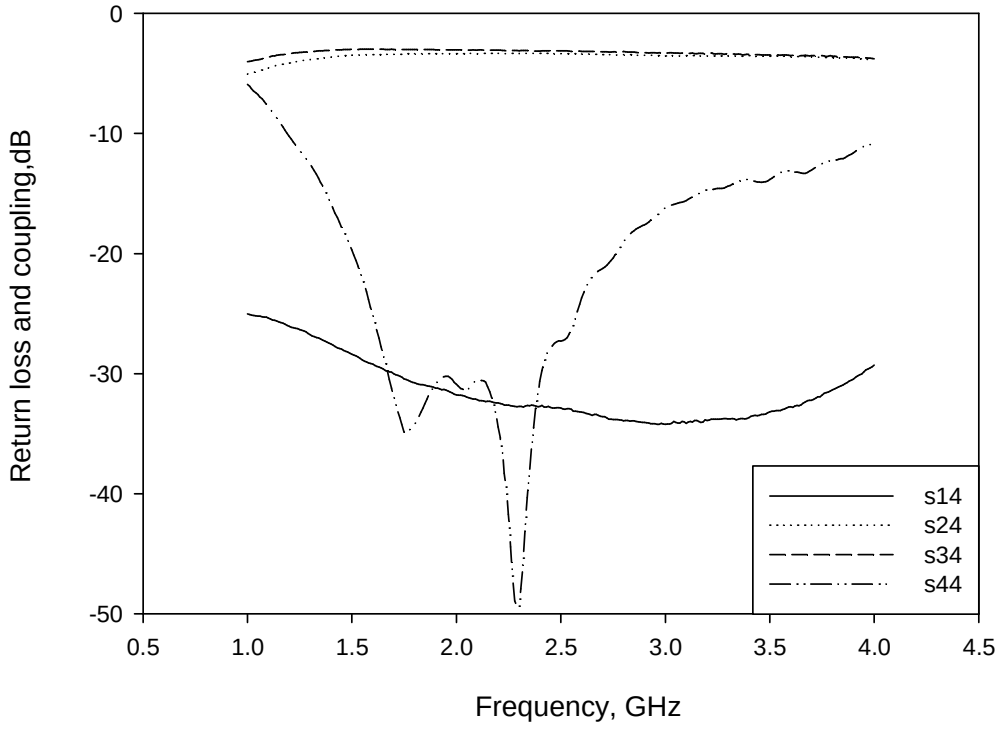

Figure 2.20: Measured amplitude response of the 180° hybrid ring for out-of-phase operation.

The amplitude and phase balance of the coupling parameters (S_{21}/S_{31}) are shown in Figure 2.21 and Figure 2.22. The amplitude and phase balance in the passband are less than 0.3dB and 3° for in-phase operation.

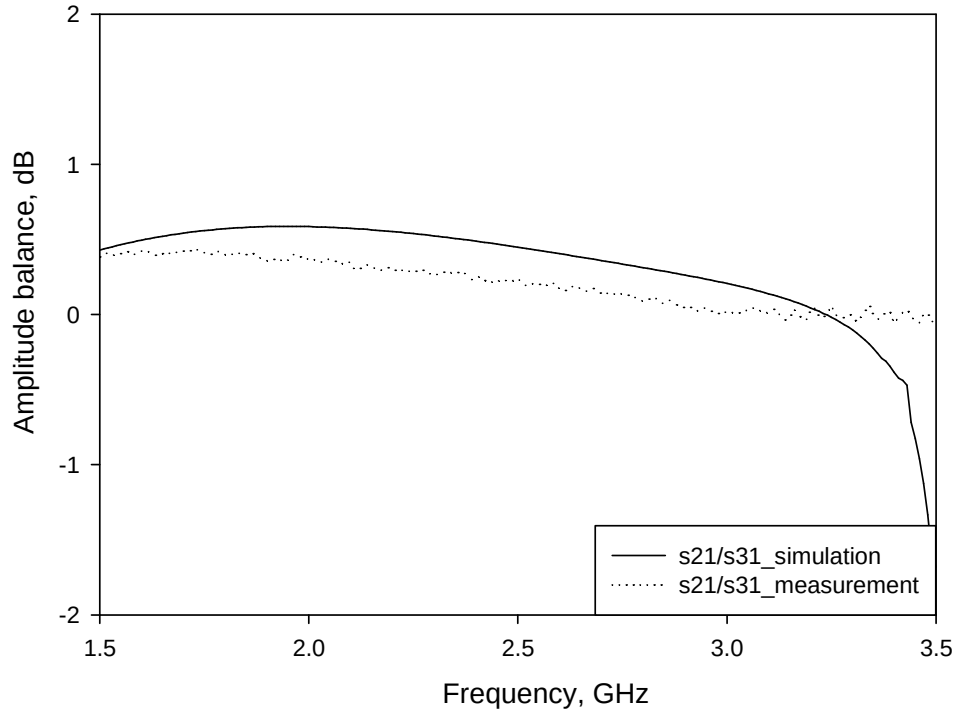

Figure 2.21: Measured amplitude balance of the 180° hybrid ring for in-phase operation.

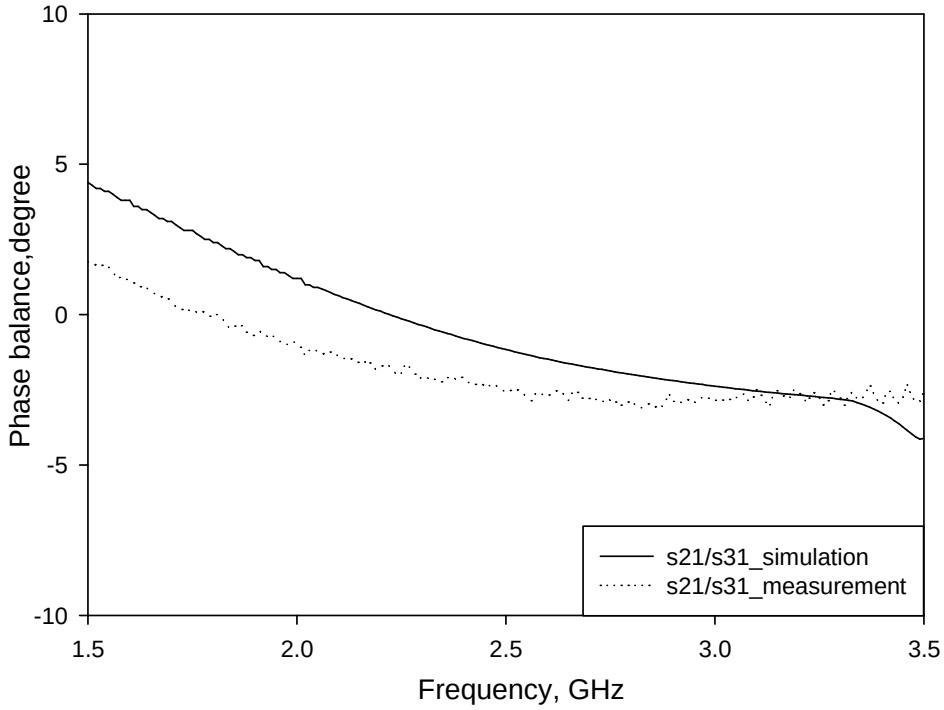

Figure 2.22: Measured phase balance of the 180° hybrid ring for in-phase operation.

The amplitude and phase balance of the coupling parameters (S_{24} / S_{34}) are shown in Figure 2.23 and Figure 2.24. The amplitude and phase balance in the passband are less than 0.5dB and 3° for out-of-phase operation.

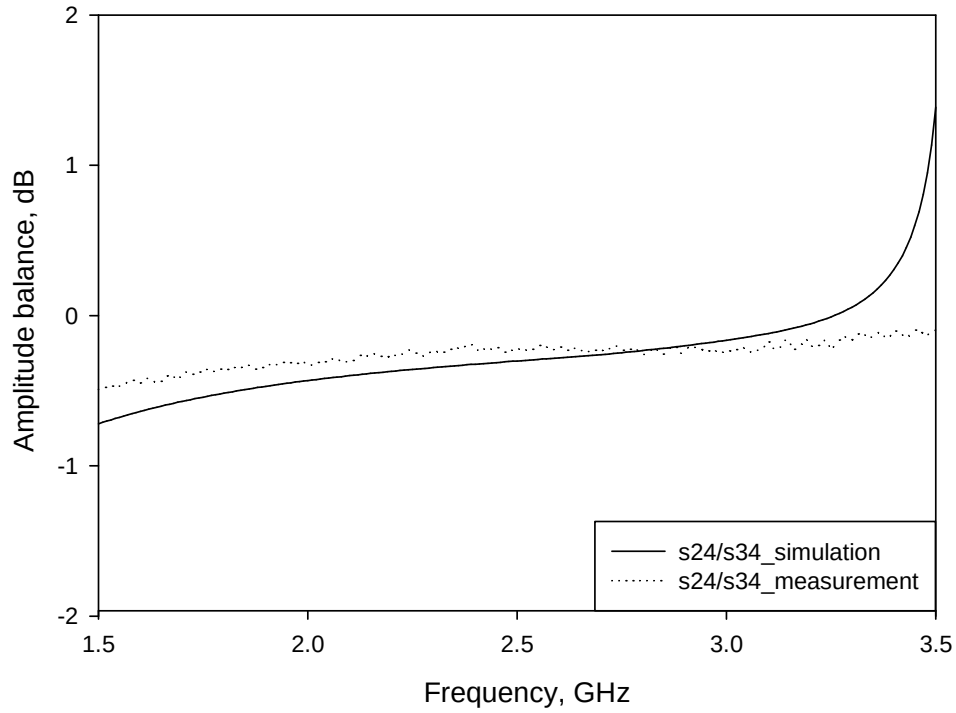

Figure 2.23: Measured amplitude balance of the 180° hybrid ring for out-of-phase operation.

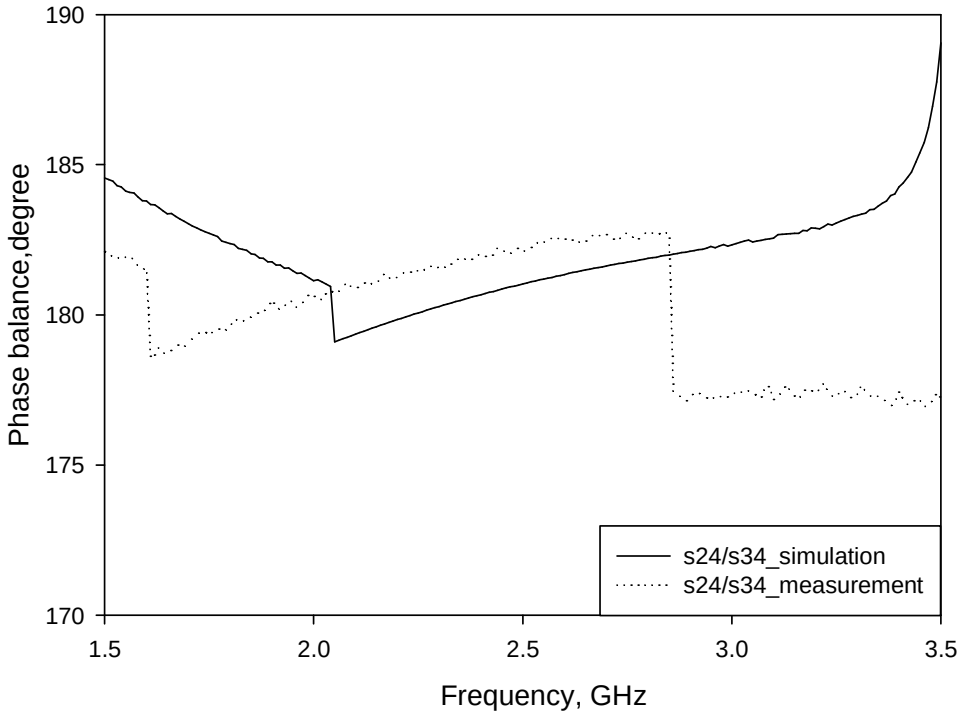

Figure 2.24: Measured phase balance of the 180° hybrid ring for out-of-phase operation.

Chapter 3
180° Reflection Type Phase Shifter

3.1 Introduction

A microwave phase shifter [9] is a device that the main function of which is to change the transmission phase of a microwave signal by means of a control or switch.

Any lumped element placed in series or shunt with a transmission line results in phase shift and, hence, there is a virtually immeasurable ways to design possible phase shifter circuit configurations. Nevertheless, adding the requirements that the device has minimum insertion loss, amplitude balance and any phase shift reduces the number of practical circuits to a little. Each offers its own combination of advantages with respect to circuit size, bandwidth and the phase shift, etc.

In order to know the working principals of the phase shifter, we need to define the special terms such as transmission phase and insertion loss first. From Figure 3.1, it can be noted that phase usually is defined using the generator voltage (V_0) phase as a reference, rather than that of the input voltage (V_1) of the system. This choice happens because that control networks are not perfectly matched; accordingly, the input voltage does not remain constant when the state of the device is changed. For practical measurement, a phase referenced to the internal voltage of the generator is

obtained by using a directional coupler to sample the forward-going wave ahead of the two port network, as shown in Figure 3.1. These couplers give output voltages proportional in amplitude and phase to V_0 and V_2, individually, even in the presence of mismatches, of course, that the coupler directivity is high enough. While the loss of a phase shifter is often overcome using an amplifier stage, the less loss, the less power amplifier that is needed to overcome it. Phase shift is the change in transmission phase of a network. Hence, we just care about relative phase shift. For instance, if a two port network has two discrete states having individual transmission phases of ϕ_1 and ϕ_2, its phase shift is $\Theta = \phi_1 - \phi_2$. The sign to be identified with Θ depends both upon which state is defined as the reference and how positive or negative phase is defined.

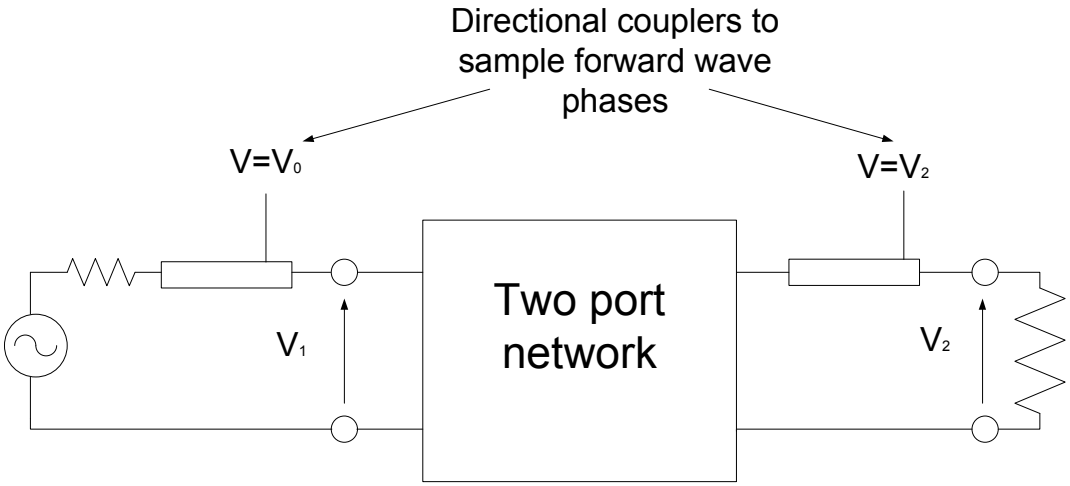

$\phi = Transmission\ phase = Argument\ of\ (V_2 / V_0)$

$IL = Insertion\ loss = 20\log_{10}(V_2 / V_0)$

Figure 3.1: Definition of transmission phase and insertion loss.

For infinitely long sinusoids, a change in θ is the same as a shift in time, such as a time delay. For example, V_2 delays by $\frac{\pi}{2}$ compared to V_0 of its cycle as shown in Figure 3.2.

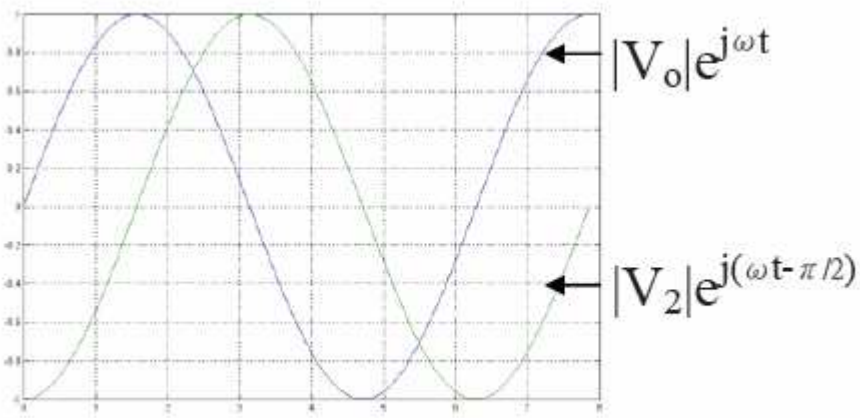

Figure 3.2: Sample sinusoid waveforms showing that a time delayed signal has negative phase.

3.2 Theory

3.2.1 Reflection Type Phase Shifter Using 90° Hybrid Coupler

There are several methods to realize phase shift by electronics. The most widespread phase shifter circuit is the one where PIN diodes (or varactors) are connected to a 3 dB 90° hybrid ring, as shown in Figure 3.3 [10]. By providing a positive or negative bias to PIN diode, two phase states can be obtained from the base elements. The range of phase shifted can be designed from a few degrees to 360 degrees.

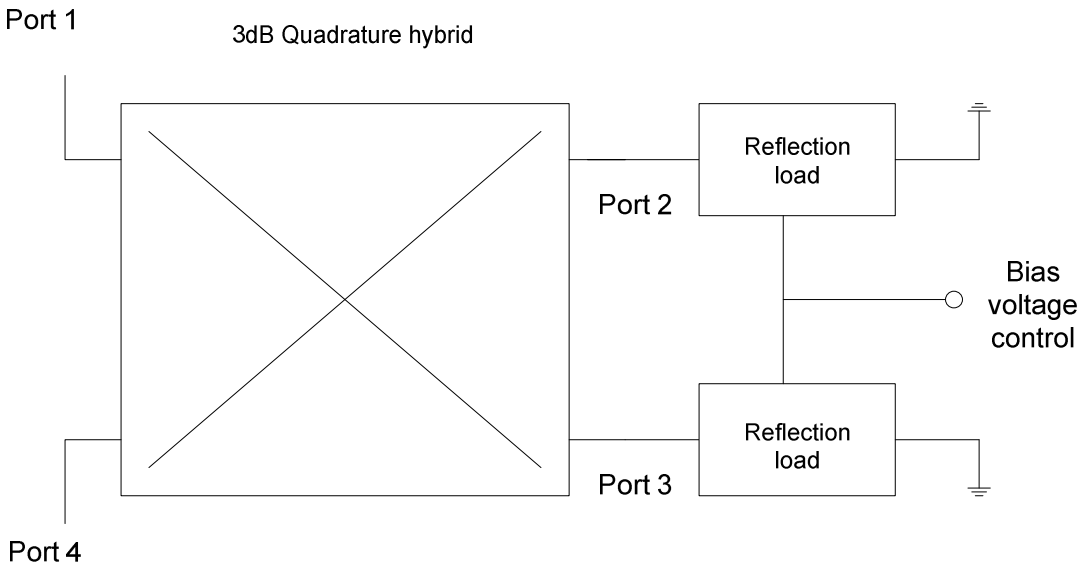

Figure 3.3: Generic reflection-type phase shifter.

The term “hybrid” has come to mean a coupler which provides a 3dB power split for the two output ports and there must be a 90° phase difference in its output signals. The scattering matrix has the following:

$$[S]=\frac{-1}{\sqrt{2}}\begin{bmatrix}0 & j & 1 & 0\\ j & 0 & 0 & 1\\ 1 & 0 & 0 & j\\ 0 & 1 & j & 0\end{bmatrix} \tag{3.1}$$

Showing that the voltage at the *i*th port as V_i by (3.1) then the relationship between V_i can be represented as follows:

$$\begin{bmatrix}V_2\\ V_3\end{bmatrix}=\begin{bmatrix}\frac{-j}{\sqrt{2}} & \frac{-1}{\sqrt{2}}\\ \frac{-1}{\sqrt{2}} & \frac{-j}{\sqrt{2}}\end{bmatrix}\begin{bmatrix}V_1\\ V_4\end{bmatrix} \tag{3.2}$$

$$\begin{bmatrix}V_1'\\ V_4'\end{bmatrix}=\begin{bmatrix}\frac{-j}{\sqrt{2}} & \frac{-1}{\sqrt{2}}\\ \frac{-1}{\sqrt{2}} & \frac{-j}{\sqrt{2}}\end{bmatrix}\begin{bmatrix}V_2'\\ V_3'\end{bmatrix} \tag{3.3}$$

In the use of phase shifting, the port 2 and port 3 should be connected with a loading circuit consisting of a PIN diode. Therefore, V_2 and V_3 caused by V_1 are reflected on the port 2 and port3.

The relationship between the signals reflected from port 2 and port 3 and the signals input to port 2 and port 3 are:

$$V_2^{'} = \Gamma V_2 = |\Gamma| V_2 e^{j\phi} \tag{3.4}$$

$$V_3^{'} = \Gamma V_3 = |\Gamma| V_3 e^{j\phi} \tag{3.5}$$

We know that $V_2^{'}$ and $V_3^{'}$ are caused by V_1. The relationship between $V_2^{'}$, $V_3^{'}$ and V_1 could be acquired by using (3.2) in (3.4) and (3.5):

$$V_2^{'} = (\frac{-j}{\sqrt{2}}) V_1 |\Gamma| e^{j\phi} \tag{3.6}$$

$$V_3^{'} = (\frac{-1}{\sqrt{2}}) V_1 |\Gamma| e^{j\phi} \tag{3.7}$$

For observing the effects of these reflected voltages on port 1 and port 4, now we can apply $V_2^{'}$ and $V_3^{'}$ in (3.6), (3.7) to (3.3), yield:

$$V_1^{'} = \frac{-j}{\sqrt{2}}(\frac{-j}{\sqrt{2}} V_1 |\Gamma| e^{j\phi}) - \frac{-1}{\sqrt{2}}(\frac{-1}{\sqrt{2}} V_1 |\Gamma| e^{j\phi}) = 0 \tag{3.8}$$

$$V_4^{'} = \frac{-1}{\sqrt{2}}(\frac{-j}{\sqrt{2}} V_1 |\Gamma| e^{j\phi}) - \frac{-j}{\sqrt{2}}(\frac{-1}{\sqrt{2}} V_1 |\Gamma| e^{j\phi}) = V_1 |\Gamma| e^{j\frac{\pi}{2} + j\phi} \tag{3.9}$$

(3.8) and (3.9) shown that, the signal inputting port 1, reflected at port 2 and port 3, is equivalent to signals $V_2^{'}$ and $V_3^{'}$ that input from port 2 and port 3 individually. The effect of two signals summing on port 1 is zero, it means no effect on port 1; however, a signal that amplitude differs from V_1 to $|\Gamma| V_1$ and phase differs by

$\phi+\frac{\pi}{2}$ at output.

If the loading circuit is made by a microstrip line with terminated by PIN diode, then, as the diode provided with positive or negative bias, marked by "*f*" or "*r*", the Γ would have a double value, noted by Γ_f and Γ_r respectively as shown in Figure 3.4. Furthermore, the ϕ also has double values, noted by ϕ_f and ϕ_r. Hence, when the PIN diodes biased positively and negatively, the output signal from port 4 should be:

$$V_{4,f}{}' = V_1 \left|\Gamma_f\right| e^{j\frac{\pi}{2}+j\phi_f} \tag{3.10}$$

$$V_{4,r}{}' = V_1 \left|\Gamma_r\right| e^{j\frac{\pi}{2}+j\phi_r} \tag{3.11}$$

The relative phase shift is:

$$\Theta = \phi_f - \phi_r \tag{3.12}$$

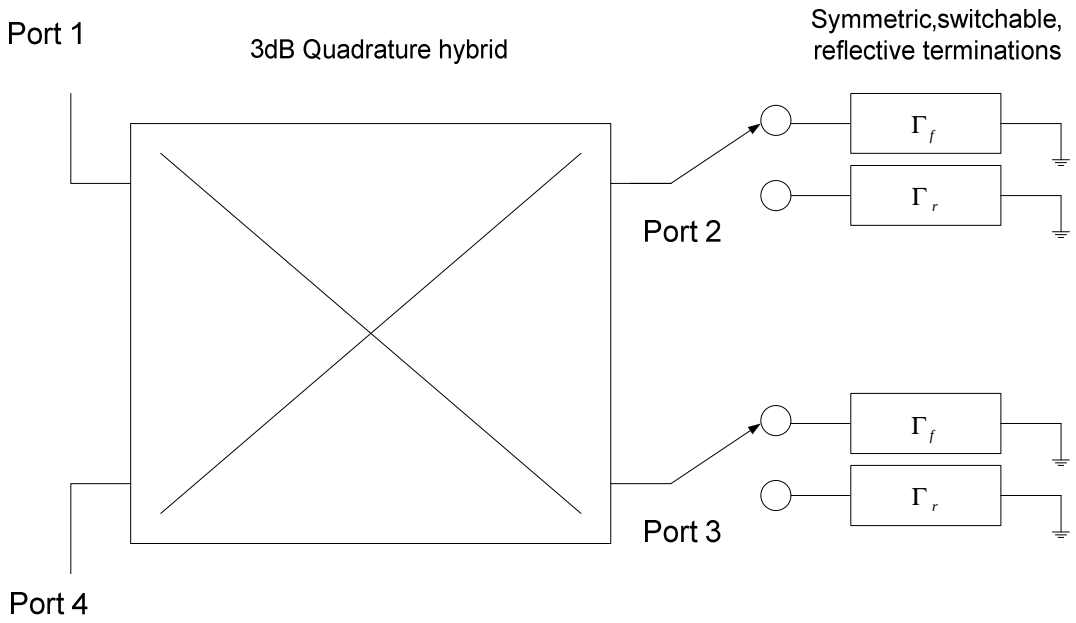

Figure 3.4: Generic reflection-type phase shifter using PIN diode.

There are many advantages of the reflection type phase shifter:

1) It only needs the least number of diodes or varactors compared to the other types of phase shifter in the use of big phase shifting.
2) Any phase shift increment can be obtained with proper design of the reflective loading circuits.
3) The transmission match of the bit is dependent only upon the design of the hybrid coupler and is separate from the design of the reflective loading circuits.
4) The reflective loading circuits can be optimized with respect to phase shift, insertion loss, amplitude balance in two bias states, or power handling capacity without regard to transmission match. In reality, it is impossible to optimize all of these functions separately in one design; hence, some compromises must be made.

3.2.2 180° Reflection Type Phase Shifter Using 180° Hybrid Ring

In this thesis, we need to realize a 180° reflection type phase shifter with the same insertion loss in two different states. However, according to (3.10) and (3.11), Γ_f and Γ_r are usually not the same. It is not proper to connect the PIN diode to a 3 dB 90° hybrid ring. We replace the 90° hybrid ring with the 180° hybrid ring, and two different loading circuits made by microstrip lines provided with positive and

negative bias, respectively. In the other state, the PIN diodes are provided with negative and positive bias as shown in Figure 3.5. By doing this, we can achieve our goal.

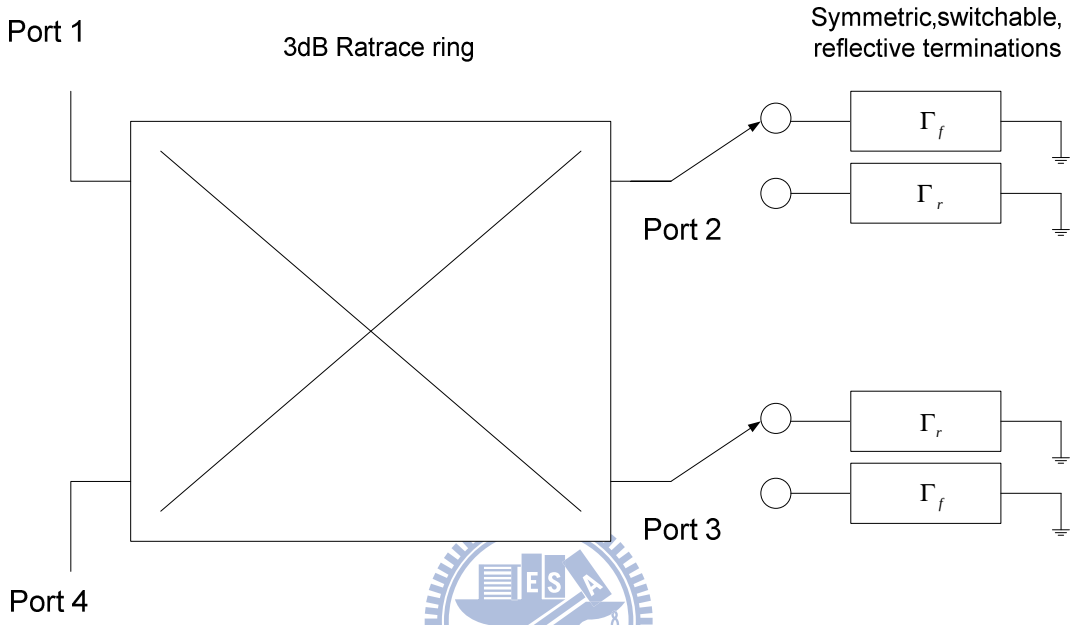

Figure 3.5: Generic 180° reflection-type phase shifter using PIN diode.

We discuss the 180° hybrid ring clearly in the previous chapter. The scattering matrix has the following:

$$[S]=\frac{-j}{\sqrt{2}}\begin{bmatrix}0 & 1 & 1 & 0\\ 1 & 0 & 0 & -1\\ 1 & 0 & 0 & 1\\ 0 & -1 & 1 & 0\end{bmatrix} \tag{3.13}$$

Showing that the voltage at the *i*th port as V_i, by (3.13) then the relationship between V_i can be represented as follows:

$$\begin{bmatrix} V_2 \\ V_3 \end{bmatrix} = \begin{bmatrix} \frac{-j}{\sqrt{2}} & \frac{j}{\sqrt{2}} \\ \frac{-j}{\sqrt{2}} & \frac{-j}{\sqrt{2}} \end{bmatrix} \begin{bmatrix} V_1 \\ V_4 \end{bmatrix} \tag{3.14}$$

$$\begin{bmatrix} V_1^{'} \\ V_4^{'} \end{bmatrix} = \begin{bmatrix} \frac{-j}{\sqrt{2}} & \frac{-j}{\sqrt{2}} \\ \frac{j}{\sqrt{2}} & \frac{-j}{\sqrt{2}} \end{bmatrix} \begin{bmatrix} V_2^{'} \\ V_3^{'} \end{bmatrix} \tag{3.15}$$

In the use of phase shifting, the port 2 and port 3 should be connected with a loading circuit consisting of a PIN diode provided with positive and negative bias. Therefore, V_2 and V_3 caused by V_1 are reflected on the port 2 and port3.

We assume the Γ of two different loading circuit are $\Gamma_f e^{j\phi_f}$, $\Gamma_r e^{j\phi_r}$ and $\phi_f - \phi_r = 180^\circ$ (We will discuss how to design in 3.3). The relationship between the signals reflected from port 2 and port3 and the signals input to port 2 and port3 are:

$$V_2^{'} = \Gamma_f V_2 = \left|\Gamma_f\right| V_2 e^{j\phi_f} \tag{3.16}$$

$$V_3^{'} = \Gamma_r V_3 = \left|\Gamma_r\right| V_3 e^{j\phi_r} \tag{3.17}$$

We know that $V_2^{'}$ and $V_3^{'}$ are caused by V_1. The relationship between $V_2^{'}$, $V_3^{'}$ and V_1 could be obtained by using (3.14) in (3.16) and (3.17):

$$V_2^{'} = (\frac{-j}{\sqrt{2}}) V_1 \left|\Gamma_f\right| e^{j\phi_f} \tag{3.18}$$

$$V_3^{'} = (\frac{-j}{\sqrt{2}}) V_1 \left|\Gamma_r\right| e^{j\phi_r} \tag{3.19}$$

For observing the effects of these reflected voltages on port 1 and port 4, now we can apply $V_2^{'}$ and $V_3^{'}$ in (3.18), (3.19) to (3.15), yield:

$$V_1^{'} = \frac{-j}{\sqrt{2}} \left[(\frac{-j}{\sqrt{2}}) V_1 \left|\Gamma_f\right| e^{j\phi_f} \right] - \frac{j}{\sqrt{2}} \left[(\frac{-j}{\sqrt{2}}) V_1 \left|\Gamma_r\right| e^{j\phi_r} \right] \approx 0 \tag{3.20}$$

$$V_4^{'} = \frac{j}{\sqrt{2}}\left[(\frac{-j}{\sqrt{2}})V_1\left|\Gamma_f\right|e^{j\phi_f}\right] - \frac{j}{\sqrt{2}}\left[(\frac{-j}{\sqrt{2}})V_1\left|\Gamma_r\right|e^{j\phi_r}\right] = \frac{1}{2}V_1\left|\Gamma_f\right|e^{j\phi_f} - \frac{1}{2}V_1\left|\Gamma_r\right|e^{j\phi_r} \tag{3.21}$$

In the other state, Γ of two different loading circuit change to and $\Gamma_f e^{j\phi_f}$ and $\Gamma_r e^{j\phi_r}$ so the relationship between the signals reflected from port 2 and port3 and the signals input to port 2 and port3 are:

$$V_2^{"} = \Gamma_r V_2 = \left|\Gamma_r\right|V_2 e^{j\phi_r} \tag{3.22}$$

$$V_3^{"} = \Gamma_f V_3 = \left|\Gamma_f\right|V_3 e^{j\phi_f} \tag{3.23}$$

The relationship between $V_2^{"}$, $V_3^{"}$ and V_1 could be obtained by using (3.14) in(3.22) and(3.23):

$$V_2^{"} = (\frac{-j}{\sqrt{2}})V_1\left|\Gamma_r\right|e^{j\phi_r} \tag{3.24}$$

$$V_3^{"} = (\frac{-j}{\sqrt{2}})V_1\left|\Gamma_f\right|e^{j\phi_f} \tag{3.25}$$

Now we can apply $V_2^{"}$ and $V_3^{"}$ in (3.24), (3.25) to (3.15), yield:

$$V_1^{"} = \frac{-j}{\sqrt{2}}\left[(\frac{-j}{\sqrt{2}})V_1\left|\Gamma_r\right|e^{j\phi_r}\right] - \frac{j}{\sqrt{2}}\left[(\frac{-j}{\sqrt{2}})V_1\left|\Gamma_f\right|e^{j\phi_f}\right] \approx 0 \tag{3.26}$$

$$V_4^{"} = \frac{j}{\sqrt{2}}\left[(\frac{-j}{\sqrt{2}})V_1\left|\Gamma_r\right|e^{j\phi_r}\right] - \frac{j}{\sqrt{2}}\left[(\frac{-j}{\sqrt{2}})V_1\left|\Gamma_f\right|e^{j\phi_f}\right] = \frac{1}{2}V_1\left|\Gamma_r\right|e^{j\phi_r} - \frac{1}{2}V_1\left|\Gamma_f\right|e^{j\phi_f} \tag{3.27}$$

(3.21) and (3.27) shown that, two different state of the phase shifter have the same amplitude and the relative phase shift is:

$$\Theta = \phi^{"} - \phi^{'} = 180^{\circ} \tag{3.28}$$

3.3 Design Procedure and Simulation

3.3.1 PIN Diode Equivalent Circuit

To realize the reflection type phase shifter, we will need an equivalent circuit for the PIN diode [11]. The PIN diode structure is a PN junction separated by an intrinsic region. Therefore comes the name P-I-N; P-type Intrinsic N-type. The PIN diode is merely an extension of the PN diode. When a forward bias is applied to the PIN, the result is a short circuit as in the PN diode. And the difference transpires when reverse biased. If the PIN diode is reverse biased, the depletion layer will increase and the junction capacitance decreases. Because of the added intrinsic region, its depletion region will be larger than the PN structure. The increased depletion width results in a smaller than normal junction capacitance when reverse biased.

Consequently, the PIN is designed to work as either forward or reverse biased. When forward biased, the series resistance ought to be as small as possible so that the diode will better represent a short circuit. When reversed biased, the junction capacitance ought to be as small as possible and close to constant over a wide range of reversed biased voltages. This allows the PIN diode to more effectively represent two distinct states; open circuit (forward bias) and short circuit (reverse bias).

The proposed equivalent circuit for the PIN diode is shown in Figure 3.6. We know that the circuit can be switched by DC to its two distinct states. In Figure 3.6,

R_f is the series resistance of the forward biased diode. When reversed biased, C_j represents the junction capacitance and R_r represents the series resistance. The parameters C_p, L_p and L_s are the elements brought by the packaging of the PIN diode. The capacitance C_p which appears in shunt is a combination of the capacitance that exists between the upper contact and the metallic ends of the semiconductor and the insulating packaging. The capacitance C_2 arises from the gap in two transmission lines across which the diode will be mounted.

Besides, all metallic ends of the package will bring about inductance, too. The inductance is divided into two components L_p and L_s. The inductance L_p appears in series with the junction capacitance. The most considerable contributions of the inductance come from the metallic contacting strap and lie on which the element is soldered. The inductance L_s accounts for the series inductance of the outlying end parts to the external contacting points. It can become very enormous if long leads are needed for bounding to the circuit.

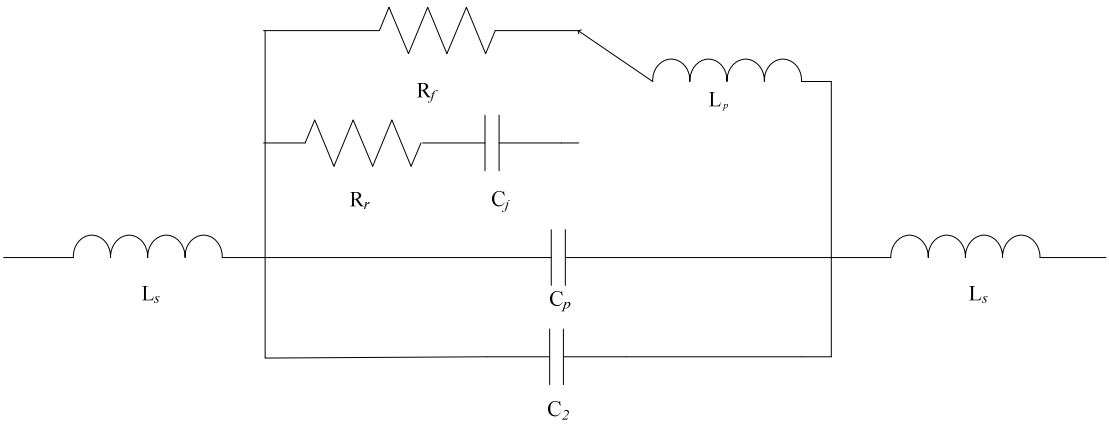

Figure 3.6: Equivalent circuit of the packaged PIN diode.

3.3.2 Tuning Procedure of Loading Circuit

In this thesis, the PIN diodes we used are the MADP-007436 Series Case Style 1279 from M/A COM Silicon Products. From the data sheet, the value for C_j is quoted as 1 pF at -20V. A typical value for R_f is 0.5 Ohms at 10 mA. The values for the package parameters can be determined from the case style considerations. A value of 0.1 pF and 0.6nH is quoted for C_p and L_s, respectively. R_r and L_p are not quoted in the data sheet.

Figure 3.7 shows two different ground structures the PIN diode mounted. The PIN diode is mounted between the microstrip line and the ground area, and its bias voltage is applied on the right side. Figure 3.7(a) shows that the top view of the ground structure composed of a fan stub which is a virtual ground. A fan stub can achieve a “perfect short” over a moderate bandwidth. Figure 3.7(b) shows a modified ground structure in order to decrease the size of the circuit. Via holes connect the top metal to the bottom, which is a metallic ground plane.

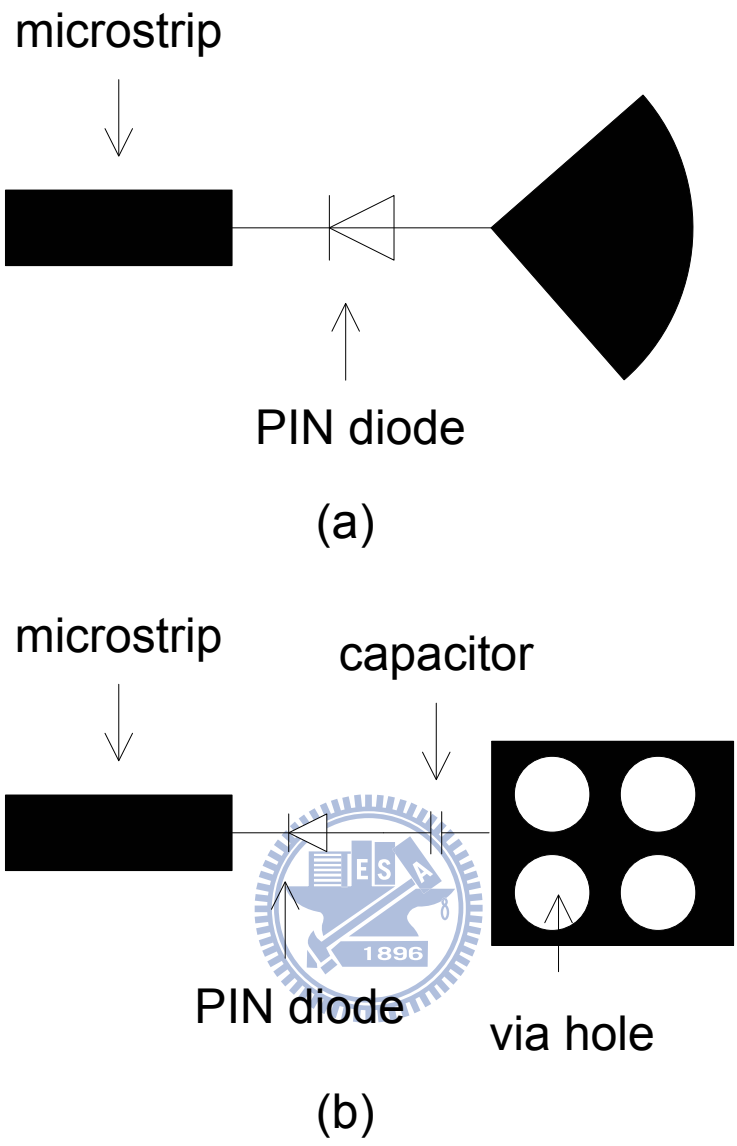

Figure 3.7: Two ground structures of the loading circuits.

Figure 3.8 illustrates the method to measure the reflection coefficient of the PIN diode at two different states (15mA and -10V). We fabricate two 50Ω microstrip lines first, the length of which are L and 2L, respectively. The former is connected to the PIN diode in series .We measure the reflection coefficient and obtain S_{11a}, and get S_{21b} from the other microstrip line. Finally, we can acquire the reflection

coefficient $R = S_{11a} / S_{21b}$. By using this method; two different coefficients in two different states can be obtained.

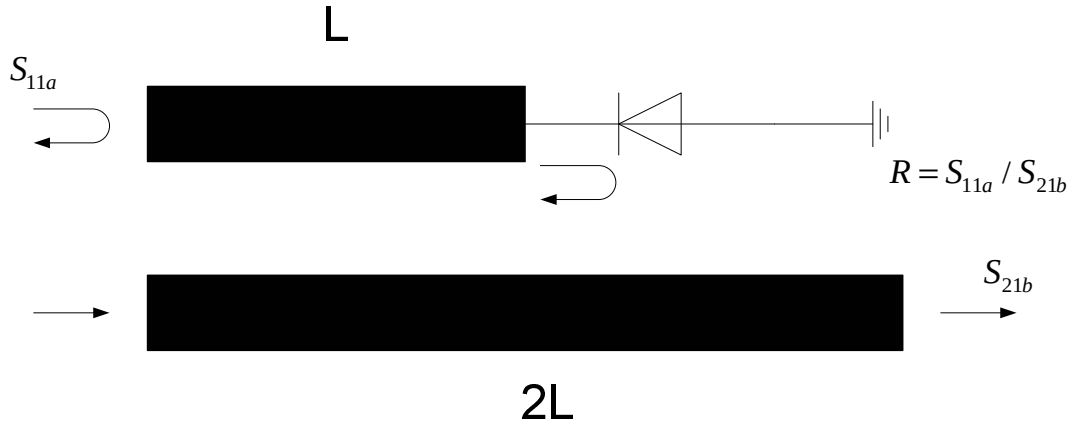

Figure 3.8: Method to measure the reflection coefficients of the PIN diode.

According to (3.20) and (3.26), in order to eliminate the term $V_1^{'}$ and $V_1^{''}$, we need to design so that the two states of the loading circuit satisfy the condition $\phi_f - \phi_r = 180^\circ$ at the center frequency. We will use two different ground structures illustrated in Figure 3.7. The ground structure of the loading circuit I is fan stub, and the other is loading circuit Π.

Take loading circuit I for example, Figure 3.9 shows the measured results of the reflection coefficients of the PIN diode. The Γ of the PIN diode is about 0.93~0.95. The initial phase shift is about 156°.

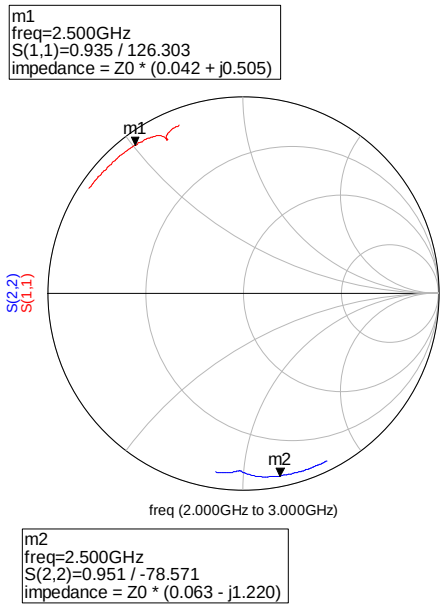

Figure 3.9: Measured results of the reflection coefficients of the PIN diode.

Now we add a 50Ω microstrip line to rotate the Γ to the condition which is symmetric to the real number axis of the Smith chart as shown in Figure 3.10.

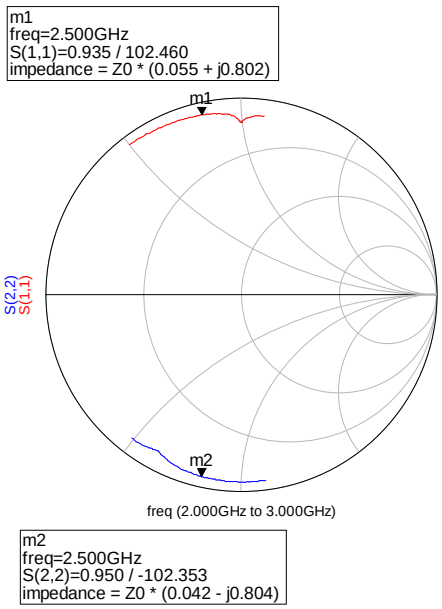

Figure 3.10: Rotation of the reflection coefficients of the PIN diode.

Finally, we add a $\frac{\lambda}{4}$ transformer to increase the phase shift to 180° at the center frequency as shown in Figure 3.11.

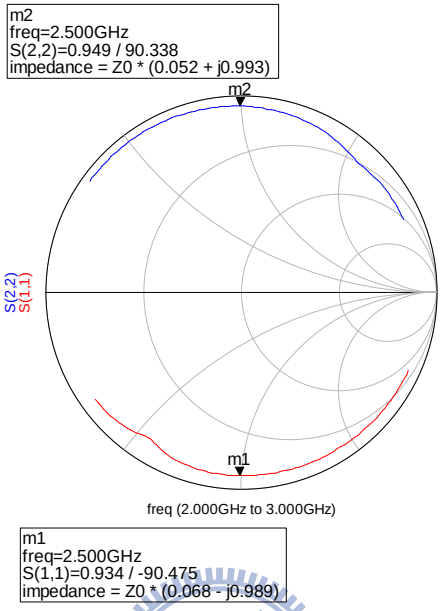

Figure 3.11: Simulated results of the reflection coefficients of the PIN diode.

The layout of the loading circuit I with physical dimensions are shown in Figure 3.12 and listed in Table 3.1.

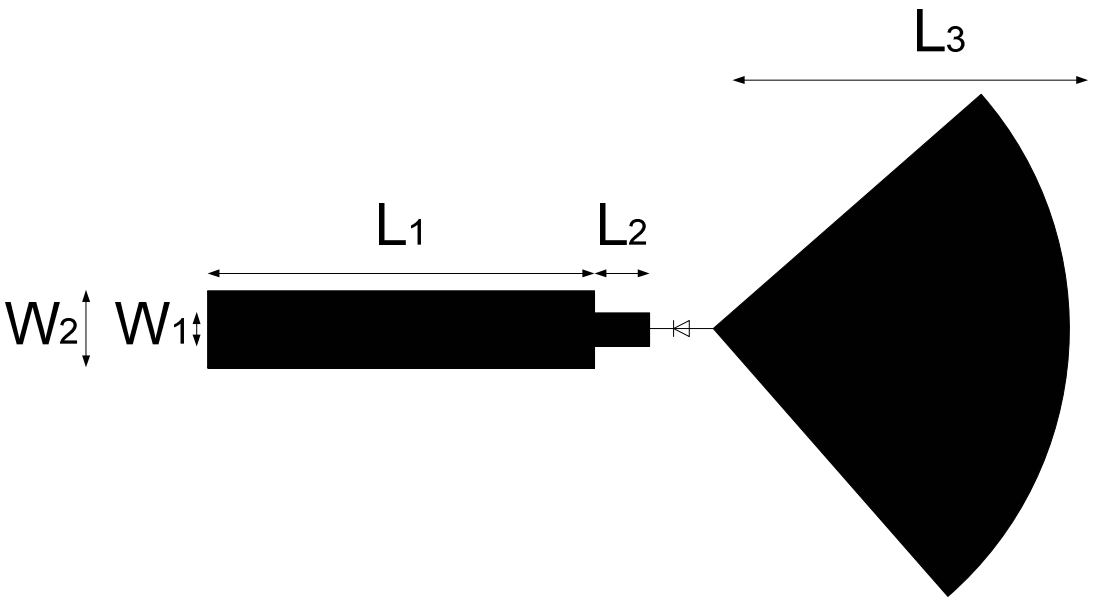

Figure 3.12: Circuit layout of the loading circuit I.

W_1(mil)	W_2(mil)	L_1(mil)	L_2(mil)	L_3(mil)
44	54	699	93	704

Table 3.1: Physical dimensions of the loading circuit I.

We can still design the loading circuit Π by the same way mentioned previously. The layout of the loading circuit Π with physical dimensions are shown in Figure 3.13 and listed in Table 3.2.

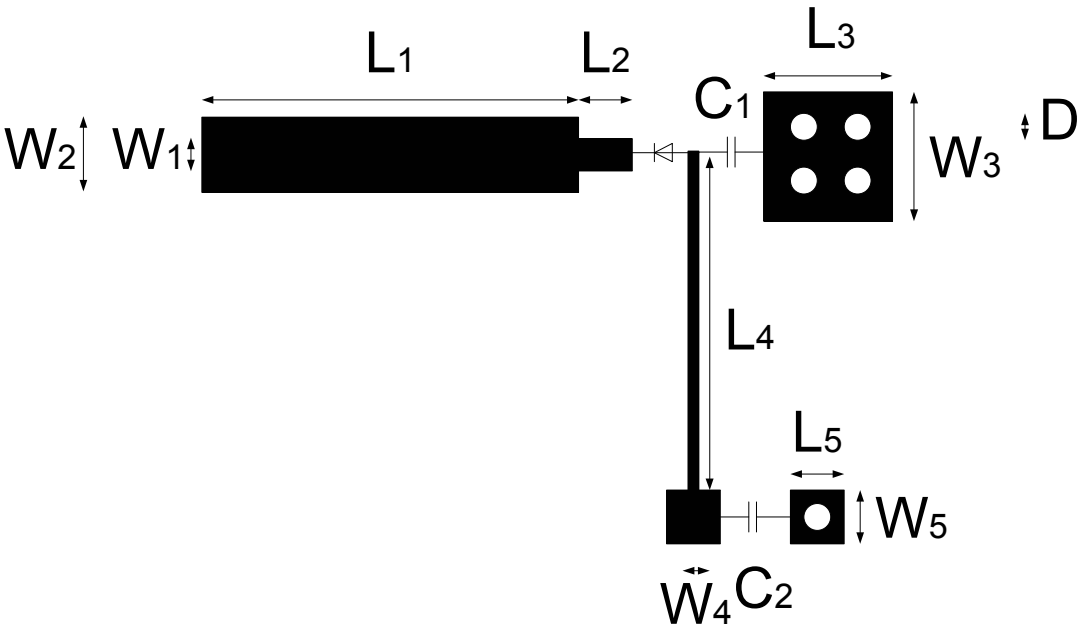

Figure 3.13: Circuit layout of the loading circuit Π.

W_1(mil)	W_2(mil)	W_3(mil)	W_4(mil)	W_5(mil)
44	62	250	6	100
L_1(mil)	L_2(mil)	L_3(mil)	L_4(mil)	L_5(mil)
695	79	250	698	100

D(mil)	C_1(pF)	C_2(pF)
40	12	18

Table 3.2: Physical dimensions of the loading circuit Π.

3.4 Fabrication and Measurements

3.4.1 Loading Circuit of 180° Reflection Type Phase Shifter

Figure 3.14 and Figure 3.15 illustrates the photograph of loading circuit I and loading circuit Π, respectively. The measured return loss responses are displayed in Figure 3.16 and Figure 3.18. It has average 0.3 dB amplitude imbalance between two states in the passband. After tuning mentioned in the previous section, two states have almost 180° phase shift at the center frequency shown in Figure 3.17 and Figure 3.19.

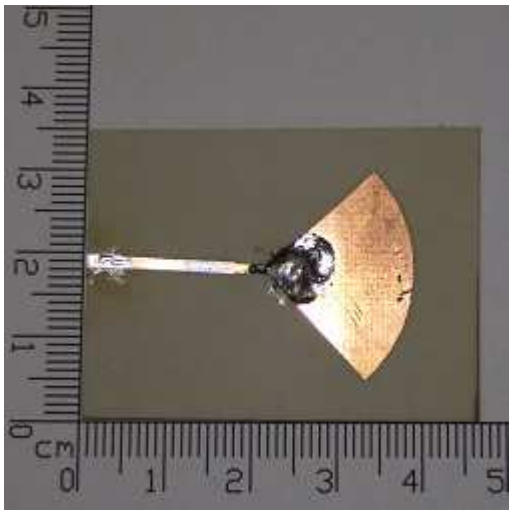

Figure 3.14: Photograph of the loading circuit I.

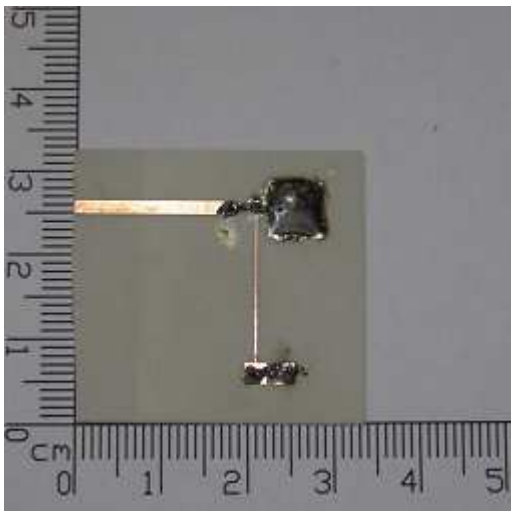

Figure 3.15: Photograph of the loading circuit Π.

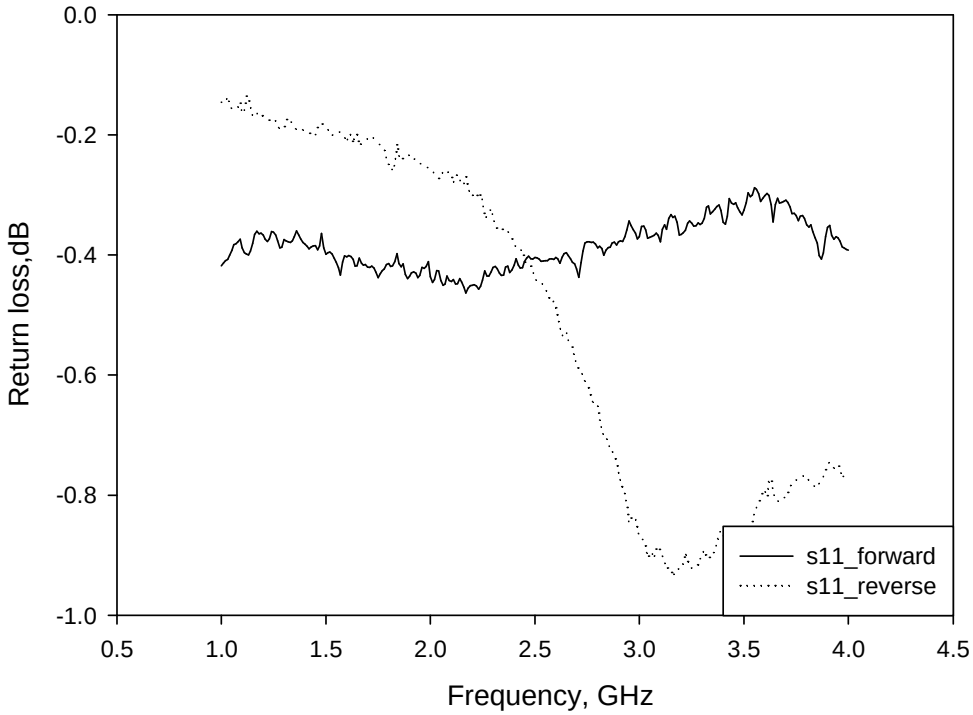

Figure 3.16: Measured amplitude response of the loading circuit I.

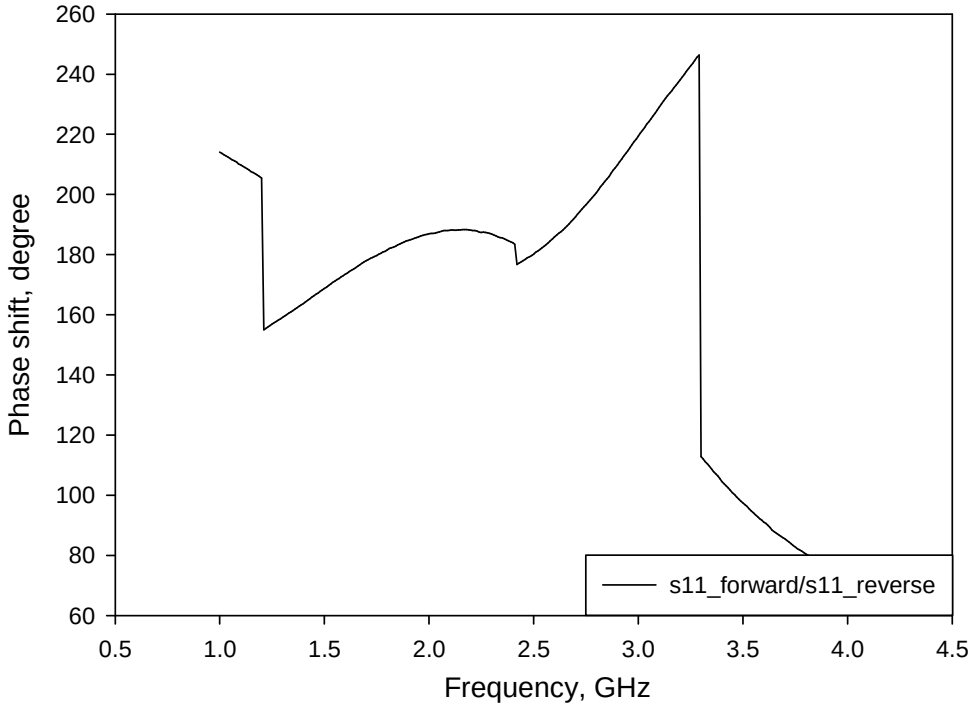

Figure 3.17: Measured phase shift of the loading circuit I.

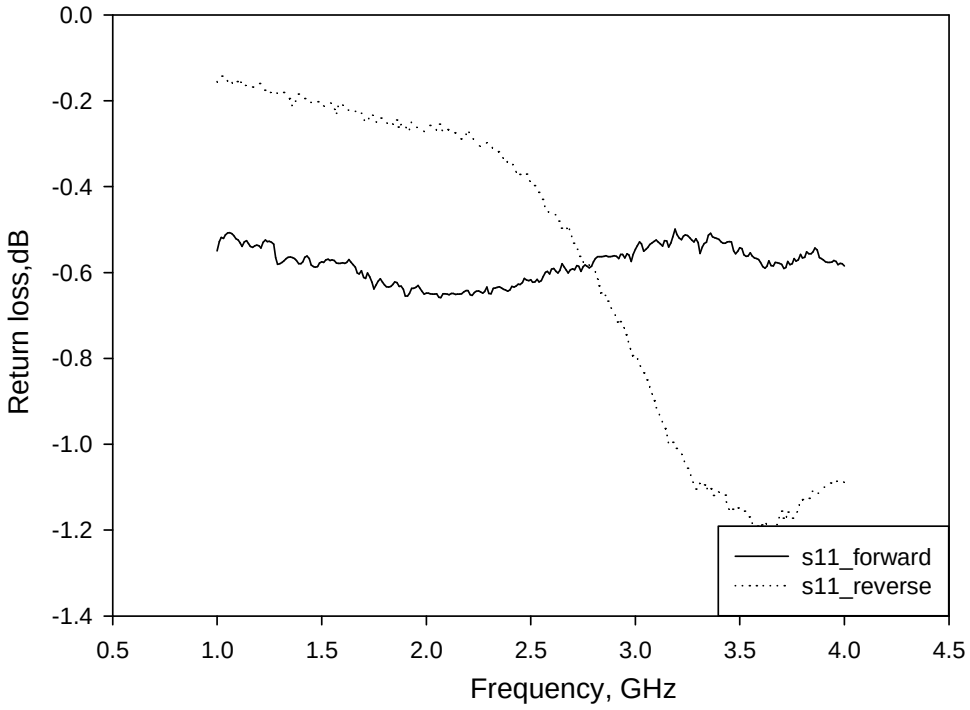

Figure 3.18: Measured amplitude response of the loading circuit Π.

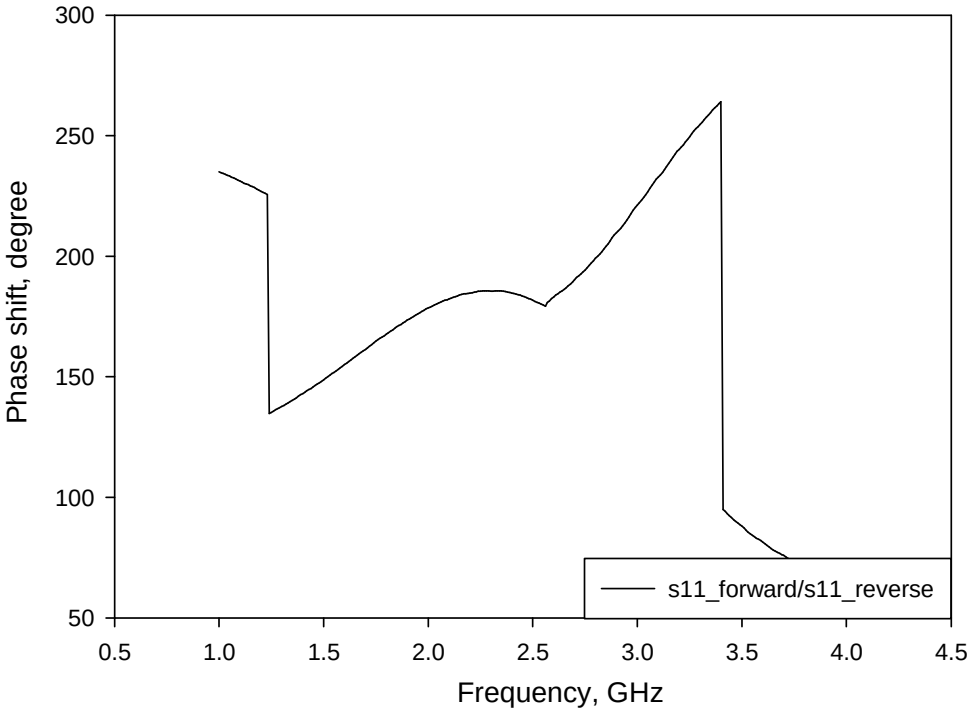

Figure 3.19: Measured phase shift of the loading circuit Π.

3.4.2 180° Reflection Type Phase Shifter

Figure 3.20 and Figure 3.21 shows the photograph of designed 180° reflection type phase shifters, which connect loading circuit I and loading circuit Π separately to the broadband 180° hybrid ring mentioned in the previous chapter. The former circuit size is 89×63 mm^2, and the latter which use reduced size ground structure is 72×68 mm^2.

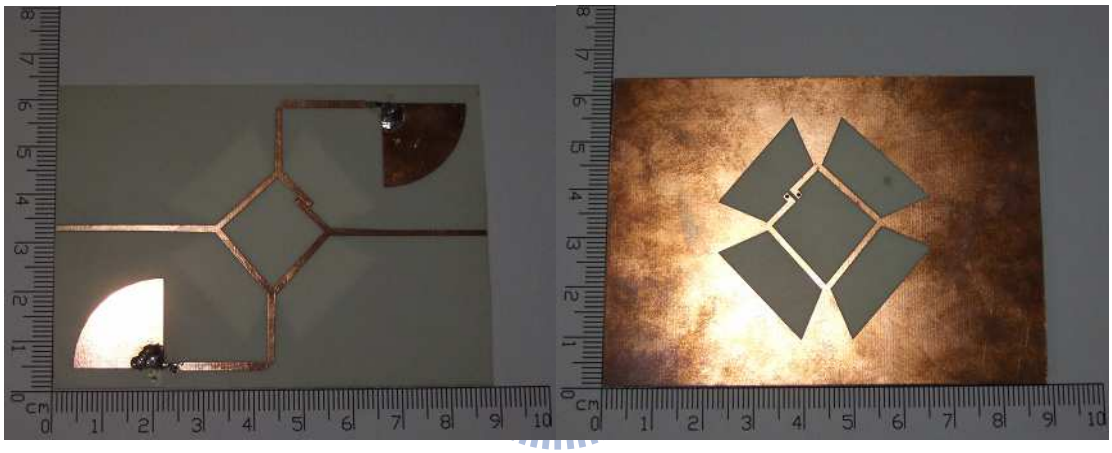

Figure 3.20: Photograph of the 180° reflection phase shifter I.

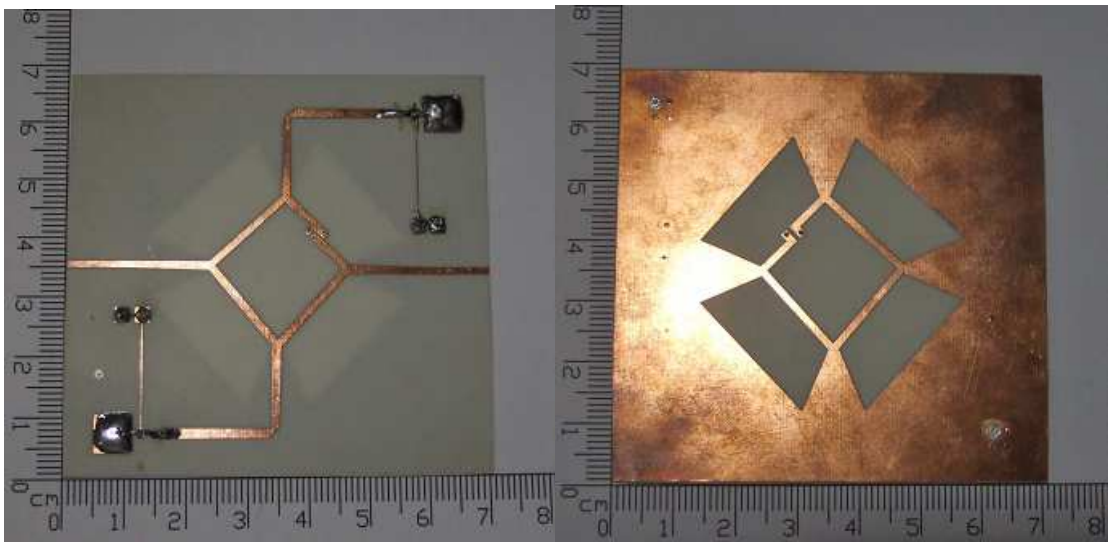

Figure 3.21: Photograph of the 180° reflection phase shifter Π.

The measured amplitude responses of the reflection type phase shifter I are shown in Figure 3.22. The return loss is better than 10 dB from 1.46 to 3.58 GHz (85%).The insertion loss is about 1.4dB.

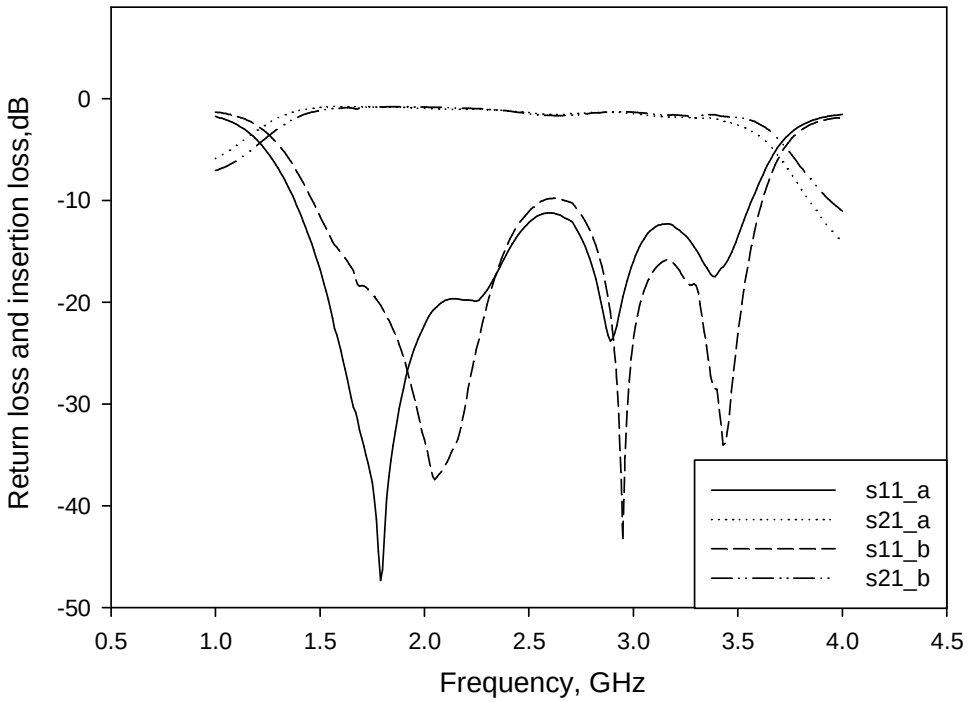

Figure 3.22: Measured amplitude response of the 180° reflection phase shifter I.

The amplitude balance and phase shift for two states are shown in Figure 3.23 and Figure 3.24. The amplitude and phase balance in the passband are less than 0.15dB and 5°.

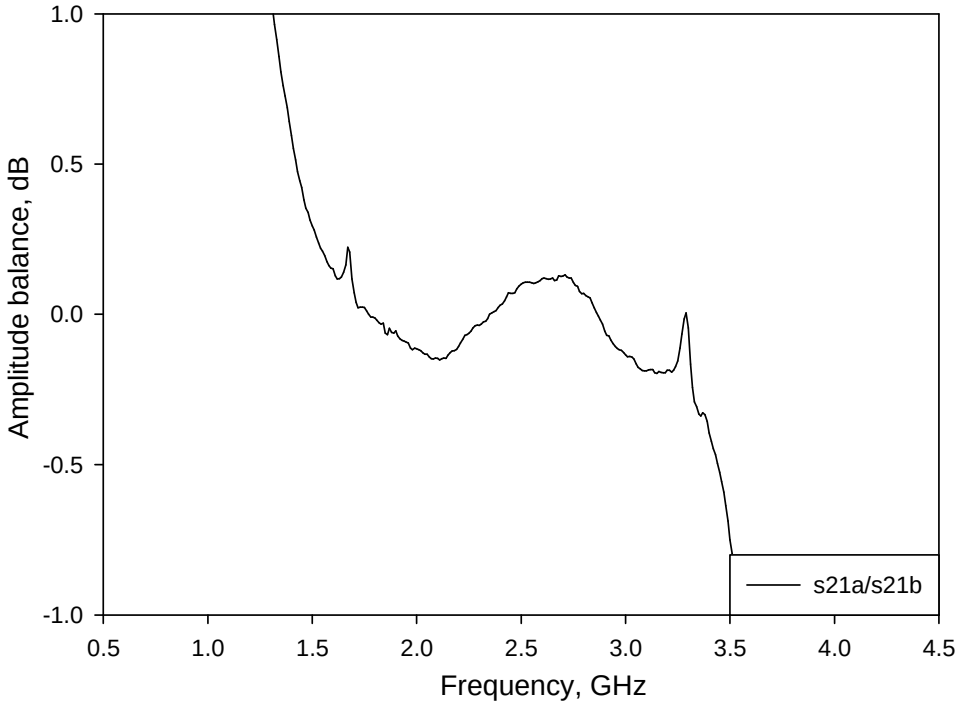

Figure 3.23: Measured amplitude balance of the 180° reflection phase shifter I.

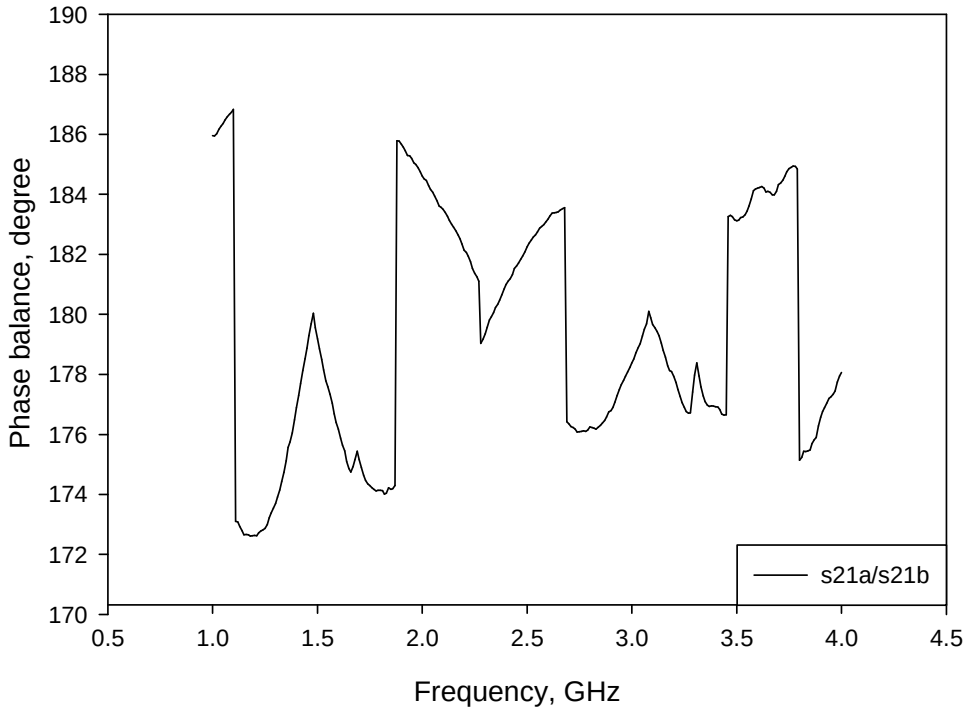

Figure 3.24: Measured phase shift of the 180° reflection phase shifter I.

The measured amplitude responses of the reflection type phase shifter Π are shown in Figure 3.25. The return loss is better than 10 dB from 1.47 to 3.47 GHz (80%).The insertion loss is about 1.3dB.

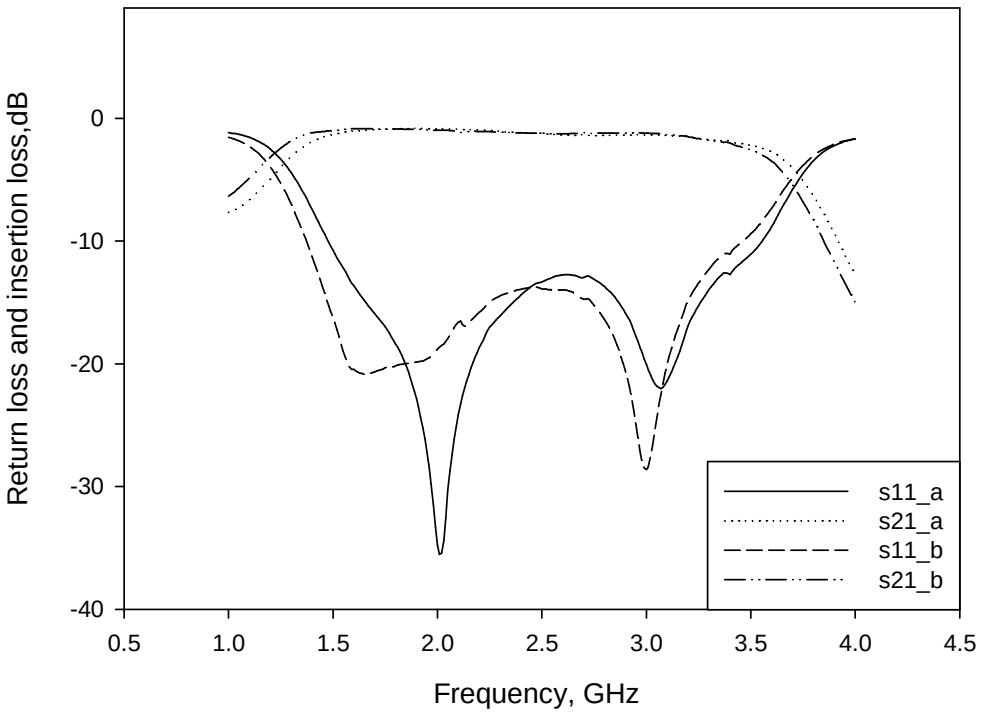

Figure 3.25: Measured amplitude response of the 180° reflection phase shifter Π.

The amplitude balance and phase shift for two states are shown in Figure 3.23 and Figure 3.24. The amplitude and phase balance in the passband are less than 0.15dB and 5°.

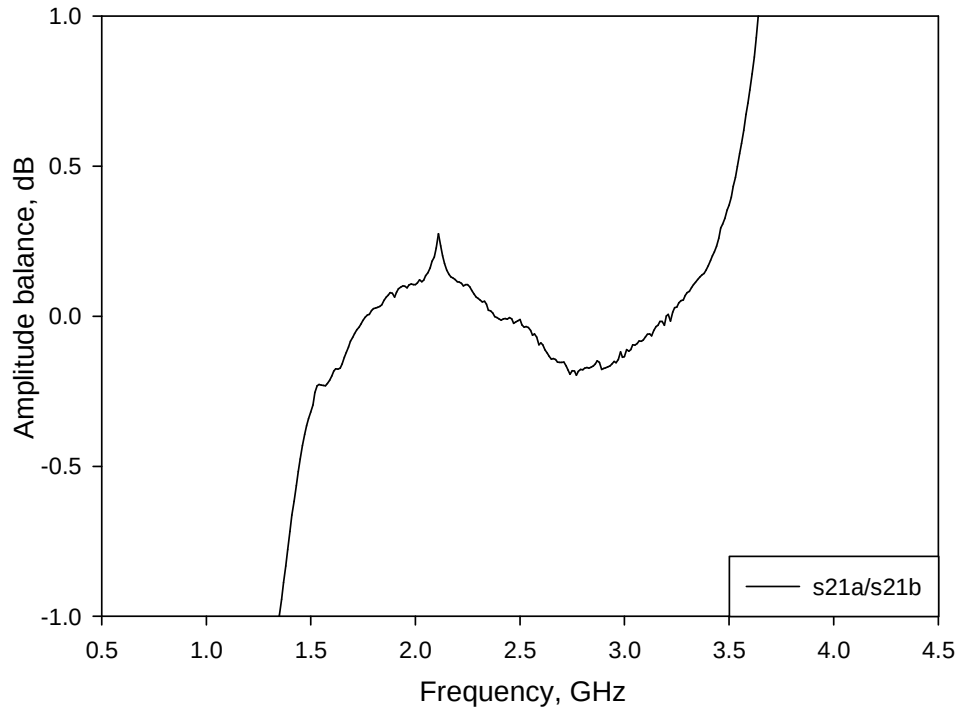

Figure 3.26: Measured amplitude balance of the 180° reflection phase shifter Π.

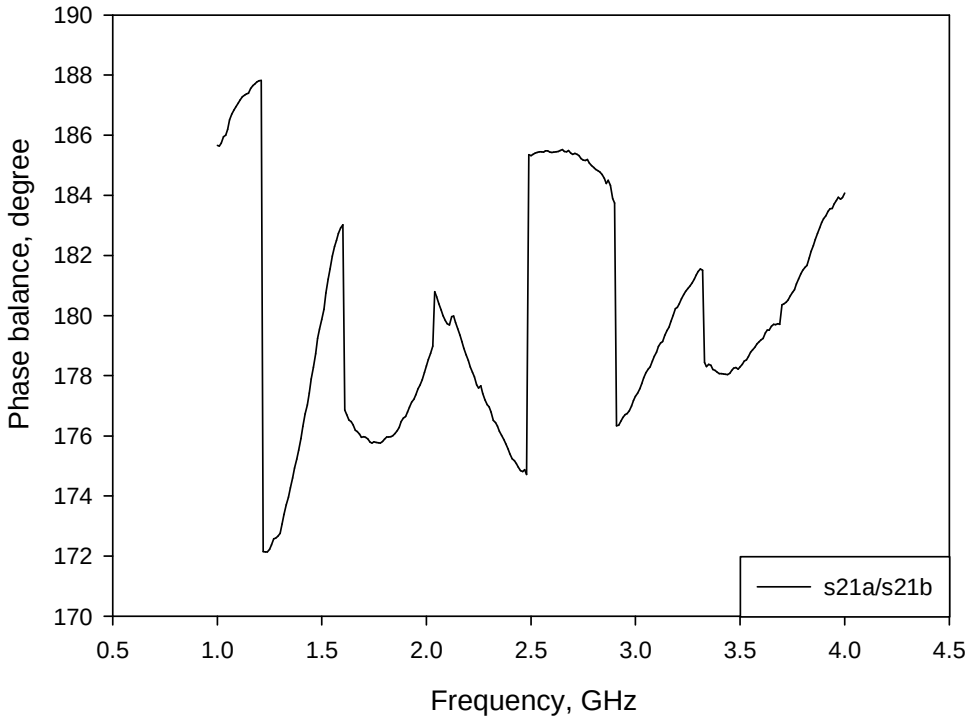

Figure 3.27: Measured phase shift of the 180° reflection phase shifter Π.

Chapter 4
Conclusion

In this thesis, the 180° reflection type phase shifters using two different ground structures were proposed. Both of the phase shifters have amplitude balance within 0.15dB and phase balance within 5° in the passband. Compared to the conventional reflection type phase shifter that we connect PIN diodes to the 90° hybrid ring, such 180° reflection type phase shifter has the minimum amplitude and phase imbalance at the broadband. In the future, we will use this useful device to be the switch of the even- and odd-mode dual band bandpass filter and the switch of the even- and odd-mode loaded line phase shifter.

A filter structure has two passbands while exciting differential or common signals is shown in Figure 4.1. In microstrip coupled lines, there are different characteristic impedances and phase velocities for even- and odd-mode signals. Using the characteristics, the filters can be realized with both stepped-impedance and uniform -impedance resonators. The two passbands can be separated effectively by adjusting the coupling strength of the coupled lines. By controlling the bias of the PIN diodes of the phase shifters, we can decide the signals we want to excite. Even- and odd-mode equivalent circuits of the dual band bandpass filter are shown in Figure

4.2(a) and (b).

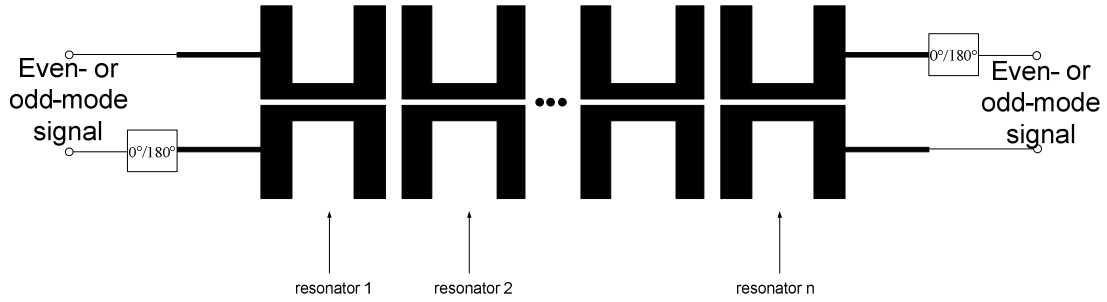

Figure 4.1: Generic even- and odd-mode dual band bandpass filter.

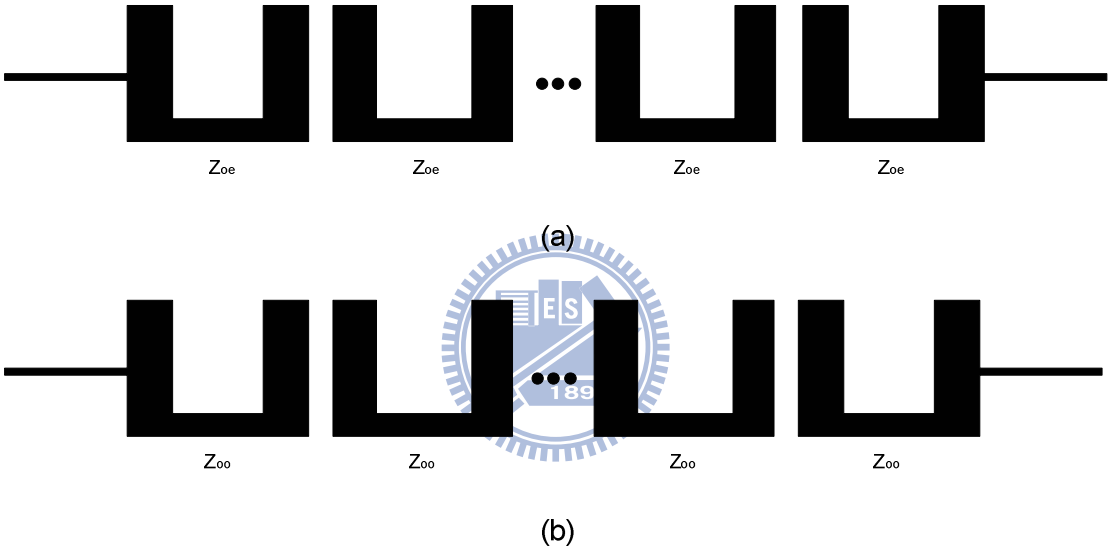

Figure 4.2: (a) Even- and (b) Odd-mode equivalent circuits of the dual band bandpass filter.

A loaded line phase shifter structure has phase shifts while exciting common or differential signals is shown in Figure 4.3. Because of the symmetry or antisymmetry of the excitation, the network can be decomposed into a set of two port networks, as shown in Figure 4.4(a) and (b). The susceptance, B, is usually implemented with an SPST PIN diode switch between two states. By exciting common or differential

signals, however, the susceptance of the load is exactly equal to the characteristic admittance of the transmission line. Without the complexity of constructing the model of PIN diode, we can easily improve the accuracy to design the loaded line phase shifter.

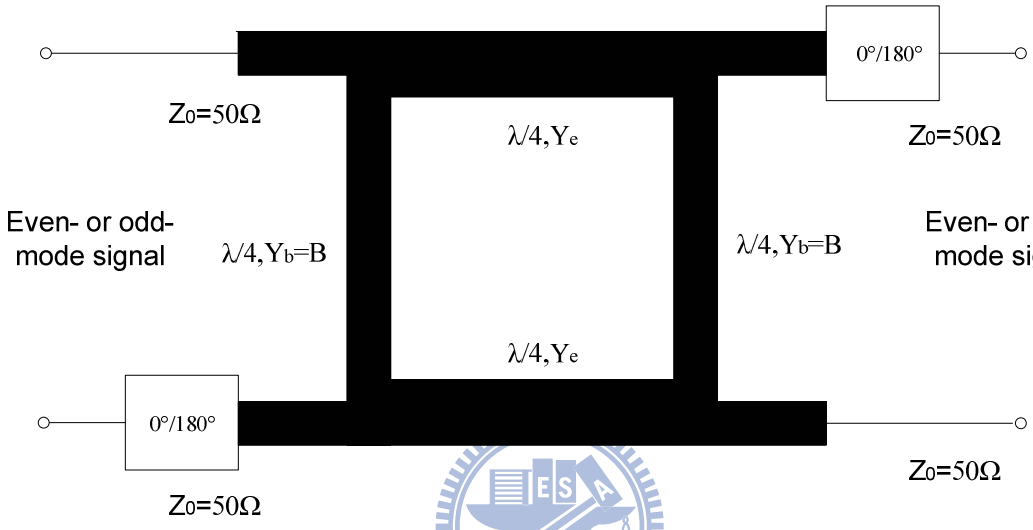

Figure 4.3: Generic even- and odd-mode loaded line phase shifter.

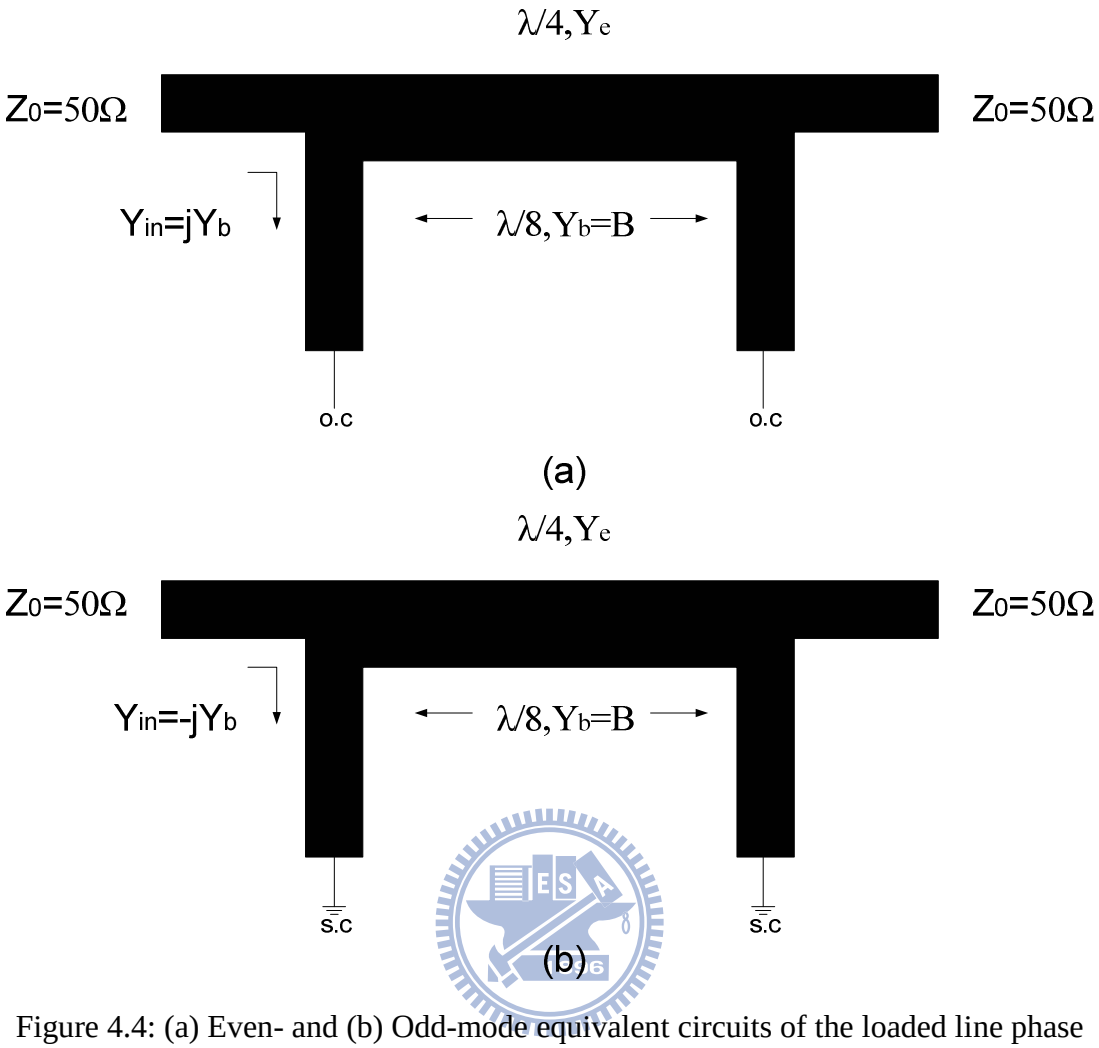

Figure 4.4: (a) Even- and (b) Odd-mode equivalent circuits of the loaded line phase shifter.

To sum up, the broadband 180° reflection type phase shifter with almost the same insertion loss can be applied in many balanced communication system, which is really a useful device in microwave engineering.

References

[1] David Pozar, *Microwave Engineering*, 3'rd Edition, John Wiley & Sons, N.Y.,2005.

[2] C.Y Chang & C.C Yang, "*A Novel Broadband Chebyshev Response Rat Race Ring Coupler*," IEEE Trans. Microwave Theory Tech., vol. 47, pp. 455–462, Apr. 1999.

[3] W.C Hong, "*Broadband Microstrip Leaky Wave Antennas*," Department of Communication Engineering, National Chaio Tung University, Ph. D Thesis, 2002

[4] Marek T. Faber & Jerzy Chramiec & Miroslaw E, *Microwave and Millimeter Wave Diode Frequency Multipliers*, Artech House, Norwood, MA, 1995.

[5] Wadell,B. C, *Transmission Line Design Handbook*, Artech House, Norwood, MA, 1991.

[6] Climer, B.J., "*Analysis of Suspended Microstrip Taper Baluns*," IEE Proc, Vol. 135, Pt. H, No. 2, pp. 65-69,Apr. 1988.

[7] Chramiec, J., & B.J.Janiczak, "*Design of Impedance Transforming Microstrip Balanced Stripline Tapered Transitions*," Electronics Letters, vol. 29, No. 1, pp. 3–4, Jan. 1993.

[8] D.J Chen, "*Design of Two Types of Ring Like Bandpass Filter with Small Size*," Department of Communication Engineering, National Chaio Tung University, Master. D Thesis, 2009

[9] White, Joseph F, *Semiconductor control*, Artech House, Norwood, MA, 1977.

[10] S.X Ming & B.Li Dong, "*Digital Phase Shifter Controlled by PIN Diode*," IEEE Trans. ICMMT., pp. 901–904, 1998.

[11] K Chang, *Microwave Ring Circuits and Antennas*, John Wiley & Sons, N.Y.,1996.

[12] C.H Wu, "*W Band Front End System for Collision Avoidance Vehicle Rader and Ku Band Analog Phase Shifter*," Department of Communication Engineering, National Chaio Tung University, Master. D Thesis, 2006

[13] W.L Chen, "*Ku Band Reflection Type Analog Phase Shifter and Reduced Size Broadband Impedance Transforming 180° Hybrid Ring Coupler*," Department of Communication Engineering, National Chaio Tung University, Master. D Thesis, 2008